horticulturae

MDPI

Article

Transcriptomic Analysis Reveals Immune Signaling Pathways Orchestrate "Lantern-like" Flower Formation Induced by *Contarinia citri* Barnes in *Citrus grandis* 'Tomentosa'

Qinqin He, Huadong Chen, Zongqin Feng, Yin Liu, Jinfeng Liu, Chun Wang * and Xinmin Huang *

Guangdong Provincial Key Laboratory for Green Agricultural Production and Intelligent Equipment, College of Biology and Food Engineering, Guangdong University of Petrochemical Technology, Maoming 525000, China; xiaohe1507@126.com (Q.H.); chd0930@163.com (H.C.); zongqinfeng@163.com (Z.F.); liu.yin@gdupt.edu.cn (Y.L.); ljfgupt@126.com (J.L.)

* Correspondence: wangchun@gdupt.edu.cn (C.W.); hxmscau@163.com (X.H.)

Abstract

Contarinia citri Barnes is a major pest of *Citrus grandis* 'Tomentosa', damaging flowers, including abnormal development with lantern-like morphology, and substantially reducing yield. However, the molecular mechanisms underlying this abnormal development remain unclear. Structural and anatomical observations combined with transcriptome analyses of normal and lantern-like flowers were performed to elucidate host regulatory pathways in response to *C. citri*. Infestation increased levels of salicylic acid, indole-3-acetic acid, and cis-zeatin, as well as chlorophyll and total flavonoid accumulation in petals. Simultaneously, an increased number of transverse petal cell layers led to petal thickening and lantern-like flower formation. Transcriptome sequencing identified 5601 differentially expressed genes. *C. citri* induced genes associated with increased petal cell number and enhanced photosynthesis and amino acid synthesis, likely providing nutrients for larvae. Most genes in the jasmonic acid, salicylic acid, and mitogen-activated protein kinase signaling pathways were up-regulated, promoting the synthesis of resistance-related compounds, including terpenoids, flavonoids, lignin, and wax, thereby enhancing petal resistance to *C. citri*. These findings elucidate plant–insect interactions and provide a new framework for understanding insect-induced plant developmental reprogramming, while identifying potential targets for breeding resistant *C. grandis* 'Tomentosa' varieties and developing novel *C. citri* control strategies.

Keywords: *Contarinia citri* Barnes; Huazhou pomelo; lantern-like flowers; differentially expressed genes; flower development

Check for updates

Academic Editor: Qian Shen

Received: 29 December 2025
Revised: 24 January 2026
Accepted: 28 January 2026
Published: 30 January 2026

Copyright: © 2026 by the authors. Licensee MDPI, Basel, Switzerland. This article is an open access article distributed under the terms and conditions of the Creative Commons Attribution (CC BY) license.

1. Introduction

Exocarpium Citri Grandis (ECG; 'Huajuhong' in Chinese) is a traditional Chinese medicinal herb that has been used for centuries as a cough suppressant, expectorant, and anti-inflammatory medication [1,2]. Experimental research shows that ECG is used to treat various diseases related to phlegm, dampness, and stagnation, including pneumonia [3], fatty liver [4], hyperlipidemia [5,6], and diabetes [7,8]. ECG can alleviate non-alcoholic fatty liver disease by reducing lipid accumulation and iron-metabolism disorders [4], and can treat hyperlipidemia by regulating the pregnane X receptor-cytochrome P450 3A4/farnesoid X receptor-liver X receptor α (PXR–CYP3A4/FXR–LXRα) pathway [5,6]. ECG is made from the fruit epicarp of *Citrus grandis* 'Tomentosa' in Huazhou, Guangdong

Province, China. At present, the planting area of Huazhou pomelo in Huazhou City has increased from 2000 ha in 2010 to 8000 ha. With the increase in planting area, the problem of pests and diseases in Huazhou pomelo is becoming increasingly serious.

Contarinia citri Barnes belongs to the gall midge family (Diptera: Cecidomyiidae) and is an important cross-regional fruit tree pest that seriously damages the flower buds of various citrus plants, including grapefruit, sweet orange, and orange [9,10]. In China, the infestation of flower bud maggots was first reported in 1953 [11]. Currently, *C. citri* has been found in major citrus production areas, such as Jiangsu, Zhejiang, Hubei, Jiangxi, Hunan, Fujian, Guangdong, and Hong Kong in China [10–12]. *C. citri* can damage flower buds (especially apical and axillary flowers) and affect fruit setting, leading to a marked reduction in fruit production and extremely serious economic consequences [10]. *Citri* has one (occasionally two) generations per year and overwinters as pupae in the soil. Adults emerge in March–April and lay eggs in blooming flower buds; the hatched larvae feed inside buds, causing abnormal flower development, failed pollination, and flower abscission. Mature larvae drop from the buds into the soil to pupate and overwinter, thereby completing the life cycle [10].

C. citri infestation of *C. grandis* 'Tomentosa' was first reported in 2008 [13]. The larvae feed on the newly developed floral organs of *C. grandis* 'Tomentosa', causing petal thickening and malformed flower buds that develop into 'lantern flowers', leading to substantial bud and flower rot. In severe cases, the proportion of damaged plants can reach over 80% of the entire orchard, severely affecting yield [13,14]. The commonly used method for preventing and controlling flower bud maggots is to use broad-spectrum insecticides, such as organophosphates and pyrethroids. However, long-term use of insecticides can cause environmental pollution, impact human health, and also lead to pest resistance [15–17]. The issue of pesticide residues in traditional Chinese medicine has attracted international attention. China, the European Union, the World Health Organization, and the United States have all introduced a series of Good Agricultural Practices to restrict the use of chemical pesticides [18,19]. Therefore, it is imperative to develop environmentally friendly and sustainable solutions to pest control. Breeding insect-resistant varieties is a long-term and effective means of preventing and controlling pest infestations in Chinese herbal medicine, and the mechanism of insect resistance is a prerequisite for cultivating highly insect-resistant medicinal plant varieties [20,21].

In response to pest attack, plants have evolved a series of defense mechanisms to protect themselves [22,23]. Upon perceiving pest infestation, plants rapidly respond through specific recognition and signaling systems and activate the expression of genes involved in secondary metabolite biosynthesis [24,25]. Plant hormones, including jasmonic acid (JA), salicylic acid (SA), ethylene (ET), abscisic acid (ABA), auxins (indole-3-acetic acid [IAA]), and cytokinins (CTK), act as crucial defense signaling systems in plants [22,23,26,27]. Among these, JA and SA and their derivatives play dominant roles by forming distinct signaling networks that regulate plant metabolism and modulate plant resistance to pests [27,28]. Chewing insects and cell-content feeders activate the plant's JA signaling pathway, whereas piercing or sucking herbivores mainly induce the SA pathway [29]. The sequential induction of JA and SA pathways at different time points can lead to synergistic effects between these hormones. This synergy enhances defense through two mechanisms. This is evidenced by, for example, repelling brown planthopper oviposition and attracting parasitoid wasps that target the planthopper larvae [30]. Insect infestation can also induce changes in the host metabolites, leading to the accumulation of nutrients required for insect growth [31]. These findings demonstrate that plant responses to herbivory involve complex regulatory mechanisms.

The formation of lantern-like flowers is a specialized response of *C. grandis* 'Tomentosa' to *C. citri*. When *C. citri* deposits eggs into developing flower buds, it causes petal thickening, a process analogous to the gall formation induced by gall midges in plant tissues [31]. This phenomenon involves the response and developmental regulation of floral organs. To our knowledge, there are currently no reports on the physiological or molecular mechanisms underlying the defense of *C. grandis* 'Tomentosa' against flower bud midge infestation, nor have such mechanisms been documented in other citrus species. This knowledge gap limits the development of new technologies for prevention and control, as well as the breeding of resistant varieties. This study used normal flowers and *C. citri*—induced abnormal flowers as material to investigate the regulatory pathways of the *C. grandis* 'Tomentosa' response to flower bud midge infestation through hormone metabolomics and transcriptomics to elucidate the molecular mechanisms underlying abnormal flower development. The findings provide insights into the genetic regulatory pathways involved in the plant's response to *C. citri* infestation, potentially informing future strategies for pest-resistant breeding.

2. Materials and Methods

2.1. Materials

Based on preliminary tracking investigations, the "Jumei" variety of *C. grandis* 'Tomentosa' exhibits more severe abnormal flower development after infestation by *C. citri* compared to other varieties. Therefore, this variety was selected as the experimental material. The plants were cultivated at the Xiangxiu Huajuhong Industrial Co., Ltd. base in Huazhou City (Maoming, China). For each biological replicate, 30 petals from normal flowers and 30 petals from *C. citri*-induced abnormal flowers of the same developmental stage were collected, pooled into one sample, immediately frozen in liquid nitrogen, and stored at −80 °C for transcriptome analysis and quantitative reverse transcription polymerase chain reaction (qRT-PCR) (Figure 1A). The study design included three biological replicates to ensure statistical robustness.

2.2. Morphological Observation

The thickness of the thickest regions of 20 normal and abnormal petals was measured using a vernier caliper. The thickest portions of the petals were then excised with a blade to prepare temporary sections. A BMC533-FLED optical microscope (Phoenix Optical, Shangrao, China) was used to observe and measure the diameters of epidermal and parenchyma cells in the transverse sections, and the number of cell layers in each transverse section was counted.

2.3. Determination of Hormone Content in Flower Petals

Petal samples (50 mg) were ground into powder in liquid nitrogen and extracted with methanol/water/formic acid (15:4:1, *v*/*v*/*v*). The combined extracts were evaporated to dryness under a nitrogen stream, reconstituted in 80% methanol (*v*/*v*), and filtered through a 0.22 μm PTFE syringe filter (Anpel, Shanghai, China). LC-ESI-MS/MS analysis was performed using an ultra-performance liquid chromatograph (UPLC) (Shim-pack UFLC SHIMADZU CBM30A system; Shimadzu, Kyoto, Japan) and the tandem mass spectrometer (MS/MS) (Applied Biosystems 6500 Triple Quadrupole; AB Sciex, Framingham, MA, USA). Chromatographic and mass spectrometric conditions followed Ge et al. [32]. Mass spectral data from different samples were processed using Analyst 1.6.1 software, integrating chromatographic peaks of all target compounds and quantifying them using reference standards. Stock solutions were prepared by dissolving standard compounds in methanol or acetonitrile. These included IAA (Sigma-Aldrich, St. Louis, MO, USA), methyl indole-3-

acetate (ME-IAA, Sigma-Aldrich, St. Louis, MO, USA), indole-3-butyric acid (IBA, Sigma-Aldrich, St. Louis, MO, USA), indole-3-carboxaldehyde (ICA, Sigma-Aldrich, St. Louis, MO, USA), N6-isopentenyladenine (IP, Sigma-Aldrich, St. Louis, MO, USA), trans-zeatin (tZ, Sigma-Aldrich, St. Louis, MO, USA), cis-zeatin (cZ, Sigma-Aldrich, St. Louis, MO, USA), dihydrozeatin (DZ, Sigma-Aldrich, St. Louis, MO, USA), methyl jasmonate (MeJA, Sigma-Aldrich, St. Louis, MO, USA), JA (Sigma-Aldrich, St. Louis, MO, USA), dihydrojasmonic acid (H_2JA, Sigma-Aldrich, St. Louis, MO, USA), ABA (Sigma-Aldrich, St. Louis, MO, USA), and SA (Sigma-Aldrich, St. Louis, MO, USA).

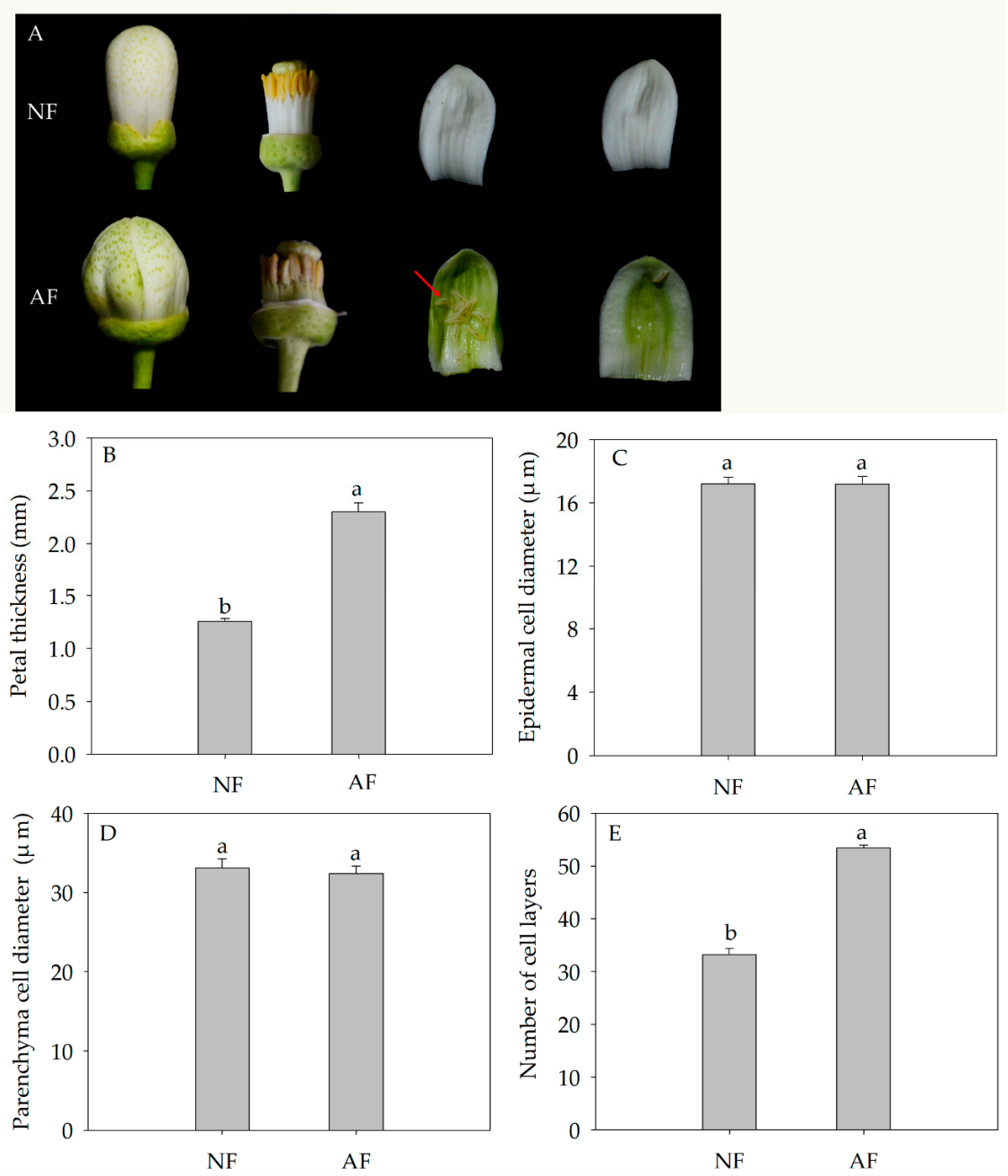


Figure 1. Observation of the morphology of *Citrus grandis* 'Tomentosa' flowers after the occurrence of *Contarinia citri* Barne infestation. (**A**): Morphology of normal and abnormal flowers. (**B**): Petal thickness of *C. grandis* 'Tomentosa' flowers. (**C**): Epidermal cell diameter. (**D**): Parenchyma cell diameter. (**E**): Number of cell layers in petal cross-sections. The red arrow indicates the *Contarinia citri* Barne larva. Different lowercase letters denote statistically significant differences (Duncan's test, $p < 0.05$). NF: Normal flowers; AF: Abnormal flowers.

2.4. Measurement of Chlorophyll Content in Petals

Uniformly sized petals of *C. grandis* 'Tomentosa' were obtained using a puncher. Approximately 0.1 g of petals was weighed, mixed with 20 mL of 95% ethanol (Hushi, Shanghai, China), and extracted in the dark for 36 h. Subsequently, the mixture was centrifuged, and 100 μL of the supernatant was taken to measure the absorbance values at wavelengths of 665 nm and 649 nm, respectively. The contents of chlorophyll a (Ca) and chlorophyll b (Cb) were calculated with reference to the method described by Lichtenthaler et al. [33].

2.5. Determination of Total Flavonoid Content in Petals

Petals of *C. grandis* 'Tomentosa' were dried to a constant weight in an oven at 60 °C, then ground into powder and passed through a 40-mesh sieve. Approximately 0.02 g of the processed sample was accurately weighed, mixed with 2 mL of 60% ethanol, and subjected to oscillatory extraction at 60 °C for 2 h. After extraction, the mixture was centrifuged at 10,000 rpm at room temperature for 10 min, and the supernatant was separated and collected. The total flavonoid content was determined at a wavelength of 502 nm using a Plant Flavonoid Detection Kit (Jiancheng Bioengineering Institute, Nanjing, China).

2.6. Transcriptome Analysis of Abnormal and Normal Flower Petals

Total RNA was extracted from each of the six petal samples using the RNeasy Plant Mini Kit (Qiagen, Valencia, CA, USA). RNA quality assessment and library construction followed the methods described previously by Huang et al. [34]. The constructed libraries were subjected to paired-end, 150 bp sequencing on the Illumina HiSeq 4000 platform (Illumina, San Diego, CA, USA). Raw sequencing reads were processed using fastp (v 0.18.0) to filter out low-quality data, followed by bowtie2 (v2.2.8) for rRNA removal, resulting in clean reads [35]. High-quality clean reads were then aligned to the *C. grandis* L. Osbeck.cv 'Wanbaiyou' v1.0 (reference genome available at http://citrus.hzau.edu.cn/download.php, accessed on 10 May 2024) using HISAT2 (v2.4) [36]. StringTie (v1.3.1) was used to reconstruct novel transcripts not included in the reference genome [37], and these novel genes were annotated using the NCBI non-redundant protein database (www.NCBI.nlm.nih.gov, accessed on 15 May 2024).

The expression levels were calculated using the FPKM (fragments per kilobase of transcript per million mapped reads) method. Principal component analysis (PCA) was conducted using the OmicShare online platform (https://www.omicshare.com/tools, accessed on 1 October 2024). The Pearson correlation coefficients of six samples were analyzed using TBtools II (v2.345). The $\log_2$ fold change (FC) was used to compare gene expression between normal and abnormal flowers [38]. When the expression level difference met the criteria of $|\log_2 FC| > 1$ and false detection rate < 0.05, the gene was considered a significantly differentially expressed gene (DEG). Specifically, $\log_2 FC > 1$ indicated up-regulated expression in abnormal flowers, whereas $\log_2 FC < 1$ indicated down-regulated expression in abnormal flowers. Gene Ontology (GO) and Kyoto Encyclopedia of Genes and Genomes (KEGG) pathway enrichment analyses were conducted to annotate the functions of DEGs.

2.7. qRT-PCR Validation of Transcriptome Sequencing Data

Total RNA was extracted from *C. grandis* 'Tomentosa' petals using the FastPure Universal Plant Total RNA Isolation Kit (Vazyme, Nanjing, China). Reverse transcription was conducted using the HiScript II Q RT SuperMix for qPCR (+gDNA wiper) kit (Vazyme). Primers for 12 DEGs were designed (Table S1), and qRT-PCR analysis was conducted using *CgActin* as the reference gene. The PCR reaction system and program followed the method

reported by Huang et al. [34], and the relative gene expression levels were analyzed using the $2^{-\Delta\Delta Ct}$ method [39].

2.8. Data Analysis

Data on petal thickness, cell diameter, number of cell layers, hormone content, and relative gene expression levels were organized using Excel 2016 (Microsoft, Redmond, WA, USA) and are presented as mean ± standard deviation. Statistical differences were analyzed using Duncan's new multiple range test, with $p < 0.05$ indicating significant differences between groups. Data visualization was performed using SigmaPlot 11 (Systat, San Jose, CA, USA).

3. Results

3.1. Observation of Abnormal Flower Development Induced by C. citri Infestation in C. grandis 'Tomentosa' "Jumei"

Hatching of *C. citri* in *C. grandis* 'Tomentosa' "Jumei" flowers induced abnormal bud development, resulting in enlarged buds with curved petals that formed a rounded, bulging "lantern-like" shape (Figure 1A). Normal flowers exhibited creamy white petals with sparse green spots, whereas unopened buds were cylindrical. In contrast, infested flowers showed dense green spots on the petals (Figure 1A). Dissection of abnormal petals indicated numerous *C. citri* larvae. Visible damage included invaded and decayed filaments/stigmas, brown filaments/anthers, shortened styles, flattened ovaries, and deformed stamens, preventing flower opening and pollination during anthesis (Figure 1A). Non-opening buds eventually wither and drop, leading to abnormal fruit setting and severe yield reduction. Using caliper measurements, infested flowers had substantially thicker petals than normal flowers (Figure 1B), indicating mite-induced petal hyperplasia. Microscopic examination revealed no statistically significant differences in the cell size of epidermal cells or middle parenchyma cells between normal and abnormal petals (Figure 1C,D). However, the number of cell layers in petal cross-sections was significantly higher in abnormal flowers than in normal flowers (Figure 1E), indicating that the increased petal thickness resulted from an increase in cell layer number rather than cell enlargement.

3.2. Differences in Hormone Contents in Petals of Normal and Abnormal Flowers

The contents of JA, SA, auxin, CTK, and ABA in petals of two different flower types were determined. The results showed that the contents of JA and its derivative MeJA in normal flowers were significantly higher than those in abnormal flowers (Figure 2). In contrast, the contents of SA, cZ, and IAA in abnormal flowers were significantly higher than those in normal flowers (Figure 2). Additionally, the contents of IBA, ICA, and ABA in normal flowers were significantly higher than those in abnormal flowers (Figure 2).

3.3. Differences in Chlorophyll Content in Petals of Normal and Abnormal Flowers

After infestation by *C. citri*, the chlorophyll content in the petals of abnormal flowers of *C. grandis* 'Tomentosa' increased. The content of Ca in abnormal flowers was 0.97 mg/g, and that of Cb was 0.83 mg/g, both of which were significantly higher than those in normal flower petals (Figure 3).

3.4. Differences in Total Flavonoid Content in Petals of Normal and Abnormal Flowers

Infestation by *C. citri* could promote the synthesis of total flavonoids in the petals of abnormal flowers of *C. grandis* 'Tomentosa'. The total flavonoid content in abnormal flowers was 76.90 mg/g, which was significantly higher than that in normal flower petals (Figure 4).

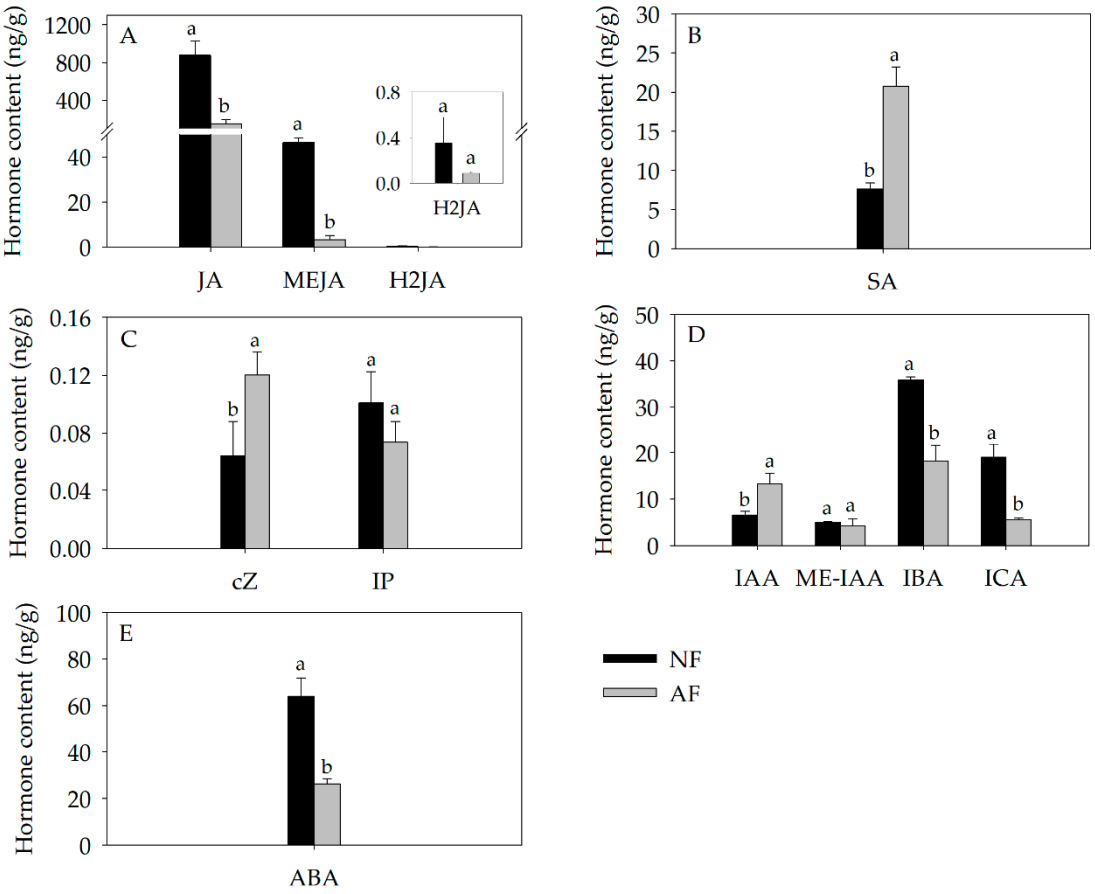


Figure 2. Different hormone contents between normal flowers and abnormal flowers. Different lowercase letters in the figure indicate statistically significant differences in hormone contents between normal flowers and abnormal flowers (Duncan's test, $p < 0.05$). (**A**): The content of Jasmonic Acid and its metabolites; (**B**): The content of Salicylic Acid; (**C**): The content of N6-isopentenyladenine and cis-zeatin; (**D**): The content of Indole-3-Acetic Acid and its metabolites; (**E**): The content of Abscisic Acid. NF: Normal flowers; AF: Abnormal flowers.

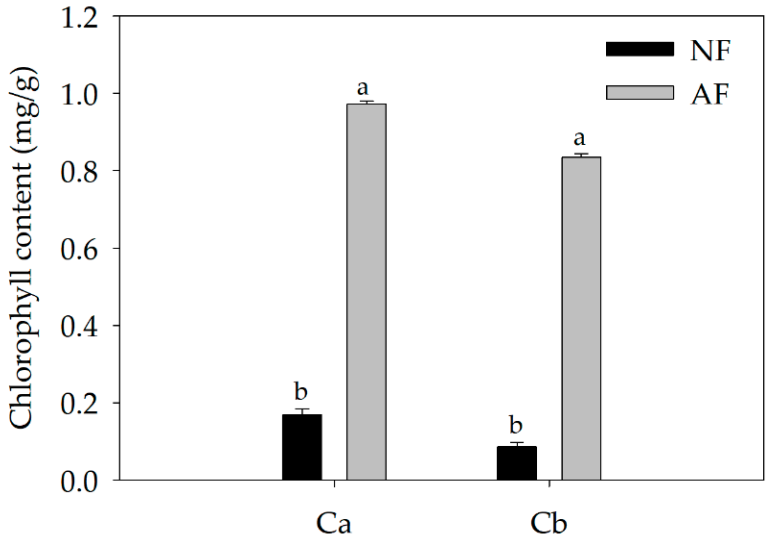


Figure 3. Contents of Chlorophyll a and Chlorophyll b in petals of normal and abnormal flowers. Different lowercase letters in the figure indicate statistically significant differences in hormone contents between normal flowers and abnormal flowers (Duncan's test, $p < 0.05$). NF: Normal flowers; AF: Abnormal flowers, Ca: Chlorophyll a, Cb: Chlorophyll b.

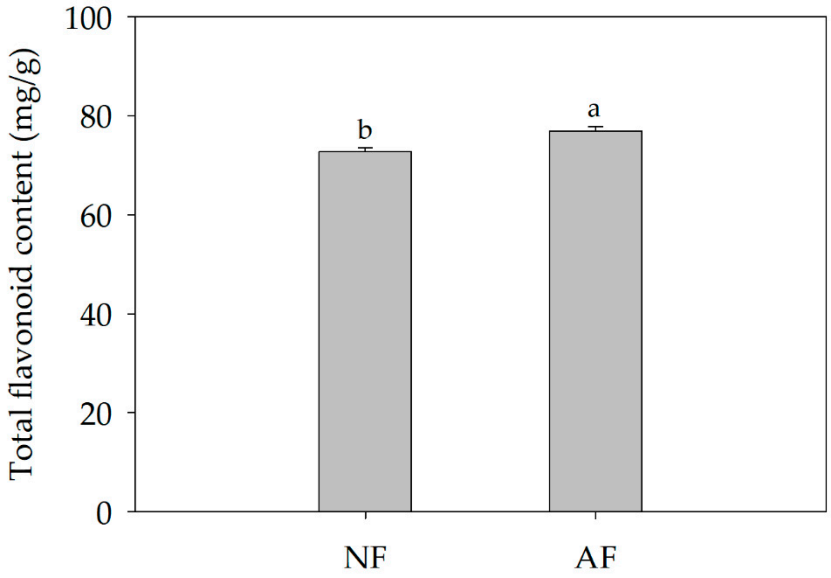


Figure 4. Total Flavonoid Content in petals of normal and abnormal flowers. Different lowercase letters in the figure indicate statistically significant differences in hormone contents between normal flowers and abnormal flowers (Duncan's test, $p < 0.05$). NF: Normal flowers; AF: Abnormal flowers.

3.5. Transcriptomic Changes Following Flower Bud Infestation

High-throughput sequencing technology was used to conduct transcriptome sequencing on normal and abnormal flower samples damaged by flower maggots. Three biological replicates were obtained for each type, and six libraries were constructed. A total of 49,401,535,099 bases were obtained (Table 1), and the Q30 (i.e., sequencing accuracy of 99.9%) of each database was greater than 91.0%. To ensure data quality, the obtained reads were filtered to remove adapters and low-quality data. The high-quality clean reads of each library were >98%, indicating high sequencing quality. High-quality clean reads were compared with rRNA databases to remove rRNA from the reads, and then the reads were compared with the pomelo genome (version 1). The alignment rate between each library and the grapefruit genome was >89.98%, with a total of 31,068 genes obtained.

Table 1. Sequencing result information table (NF: Normal flowers; AF: Abnormal flowers).

Sample	Raw Data (bp)	Clean Data (bp)	Q30 (%)	Removed rRNA (%)	Mapped Reads (%)	Known Genes Number	Novel Transcripts Number	All Genes Number
NF1	7,034,891,100	7,009,089,308	92.19	93.86	95.56	19,498 (64.73%)	874	20,372
NF2	8,693,667,000	8,648,820,401	91.73	96.53	95.48	19,984 (66.34%)	903	20,887
NF3	10,041,009,600	9,964,733,975	93.69	88.71	95.56	19,637 (65.19%)	899	20,536
AF1	8,587,471,500	8,526,574,218	94.43	95.15	89.98	18,833 (62.52%)	880	19,713
AF2	7,984,127,100	7,959,607,589	93.21	95.67	93.93	19,336 (64.19%)	898	20,234
AF3	7,313,641,800	7,292,709,608	93.46	92.68	90.00	18,783 (62.35%)	908	19,691
Total	49,654,808,100	49,401,535,099				21,835	945	22,780

Comparing the annotation of genes in the genome of the pomelo, 21,835 genes were identified as known genes in the genome, with 19,498, 19,984, 19,637, 18,833, 19,336, and

18,783 genes in six libraries, respectively. A total of 945 new transcripts (874, 903, 899, 880, 898, 908 in six libraries) were identified (Table 1).

PCA was conducted on the FPKM values of the six samples. The normal and abnormal flowers were clearly separated along the PC1 axis (Figure 5A), indicating statistical differences in gene expression between the two types of petals. Pearson correlation coefficients of the FPKM values of the six samples indicated a very low correlation between abnormal and normal flowers. The Pearson correlation coefficients among the three replicates of the same petal type were all >0.90 (Figure 5B), indicating high reproducibility of the sequencing and suitability for subsequent differential expression analysis.

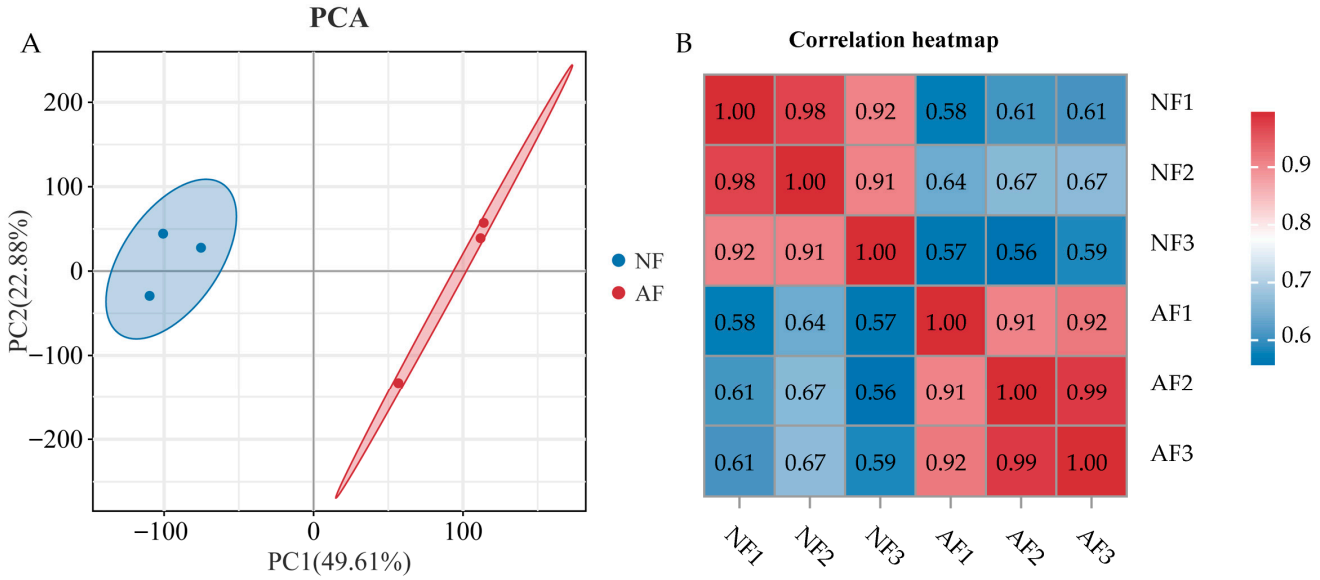


Figure 5. Principal component analysis (PCA) and correlation analysis of transcriptome sequencing results of normal and abnormal flowers. (**A**): PCA; (**B**): Correlation analysis, the numbers in the figure represent Pearson correlation coefficients. NF: Normal flowers; AF: Abnormal flowers.

3.6. Screening and Enrichment Analysis of DEGs Between Normal and Abnormal Flowers

Log_2FC was used to screen for DEGs; the differences in gene expression between normal and abnormal flowers are shown in Figure 6A. Further screening indicated a total of 5601 DEGs, with 4044 genes up-regulated and 1557 genes down-regulated in the abnormal flowers (Figure 6B).

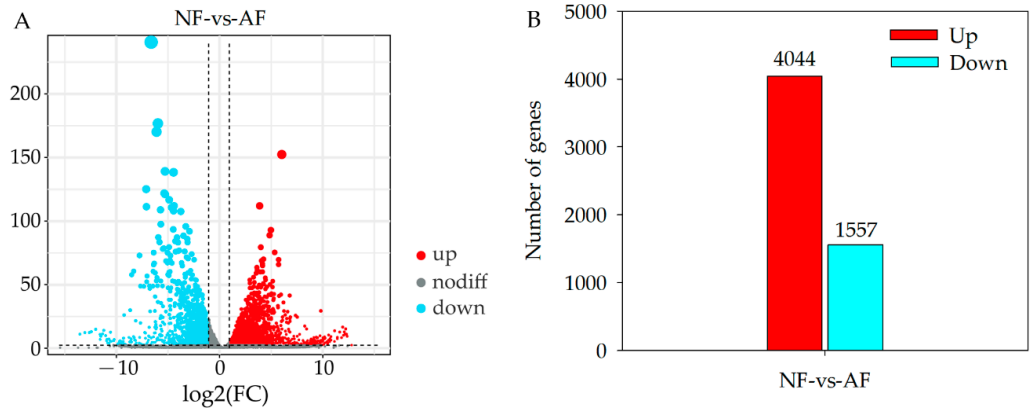


Figure 6. Differential gene analysis of *Citrus grandis* 'Tomentosa' flowers after the occurrence of *Contarinia citri* Barne infestation in flower buds. (**A**): Volcano plot of differential genes; (**B**): The number of differential genes; NF: Normal flowers; AF: Abnormal flowers.

KEGG analysis was conducted to identify the metabolic pathways enriched in the up- or down-regulated DEGs. A total of 842 up-regulated DEGs were mapped to 141 pathways, of which 18 pathways were significantly enriched (Figure 7A; Table S2). The pathways with the highest number of enriched DEGs were metabolic (ko01100, 517 DEGs), biosynthesis of secondary metabolites (ko01110, 333 DEGs), plant hormone signal transduction (ko04075, 86 DEGs), carbon metabolism (ko01200, 55 DEGs), phenylpropanoid biosynthesis (ko00940, 44 DEGs), glycolysis/gluconeogenesis (ko00010, 37 DEGs), and pyruvate metabolism (ko00620, 28 DEGs).

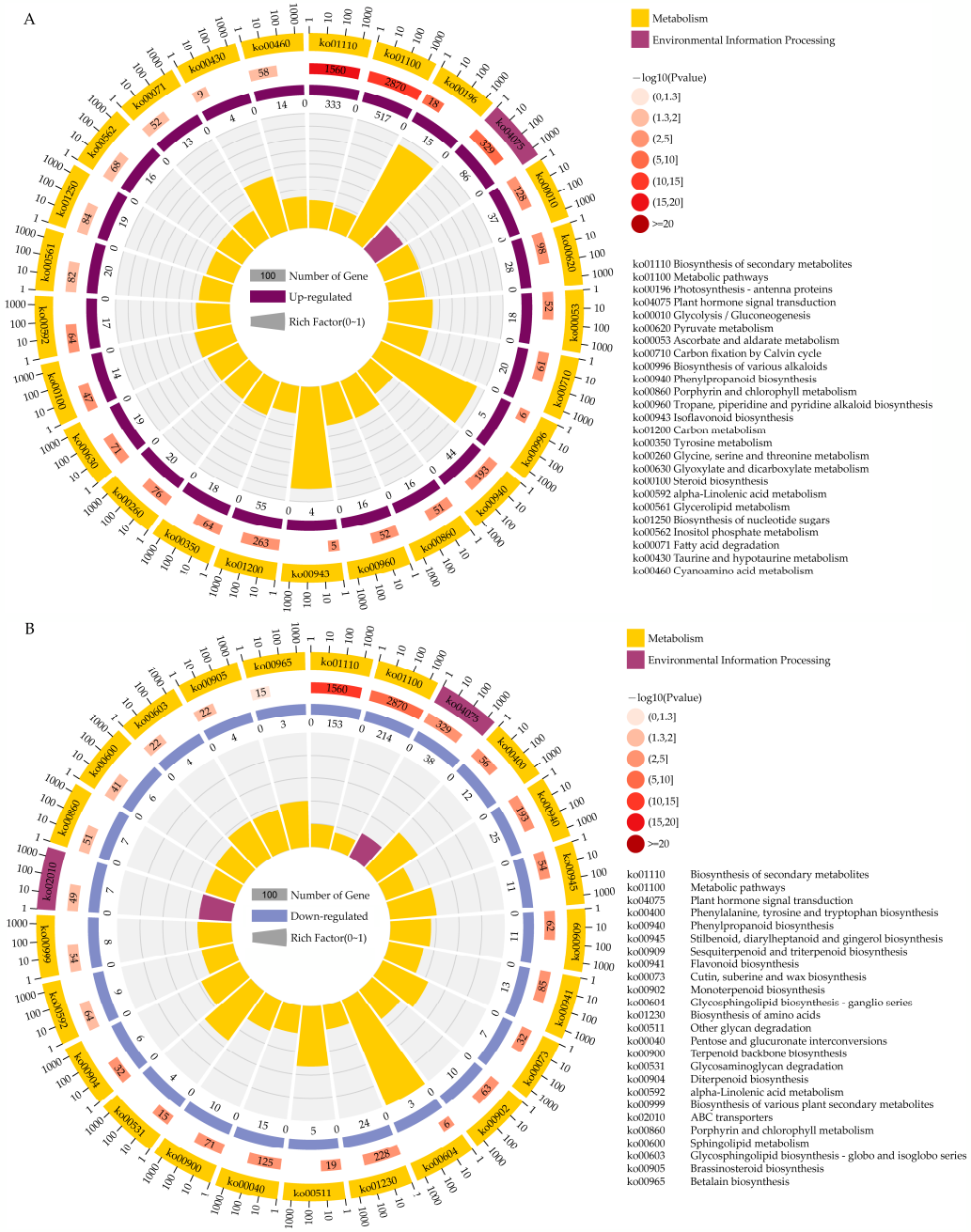


Figure 7. Top 25 KEGG pathways enriched among up-regulated (**A**) and down-regulated (**B**) differentially expressed genes. The innermost bar chart represents the enrichment factor for each pathway, defined as the ratio of differentially expressed genes to the total number of genes annotated in that pathway.

Of the 18 significantly enriched pathways, eight were related to photosynthesis and carbon metabolism, including photosynthesis—antenna proteins (ko00196), glycolysis/gluconeogenesis (ko00010), pyruvate (ko00620), ascorbate and aldarate (ko00053), porphyrin and chlorophyll (ko00860), carbon (ko01200), and glyoxylate and dicarboxylate metabolism (ko00630), and carbon fixation by Calvin cycle (ko00710).

A total of 345 down-regulated DEGs were mapped to 121 metabolic pathways, of which 13 pathways were significantly enriched (Figure 7B; Table S3). The pathways with the highest number of DEGs were biosynthesis of secondary metabolites (ko01110, 153 DEGs), metabolic pathways (ko01100, 214 DEGs), plant hormone signal transduction (ko04075, 38 DEGs), phenylpropanoid biosynthesis (ko00940, 25 DEGs), and biosynthesis of amino acids (ko01230, 24 DEGs). These 13 significantly enriched pathways were primarily associated with the biosynthesis of flavonoids, terpenoids, and other secondary metabolites.

GO analysis indicated that a total of 330 up-regulated DEGs were enriched in the Cellular Component category, with significant enrichment in membrane part (GO:0044425, 178), membrane (GO:0016020, 200), intrinsic component of membrane (GO:0031224, 154), and photosystem I (GO:0009522, 7) (Figure 8A; Table S4). A total of 881 up-regulated DEGs were enriched in the Molecular Function category, enriched in GO terms related to enzyme activity regulation, including oxidoreductase (GO:0016491, 182), protein kinase (GO:0004672, 97), phosphotransferase, alcohol group as acceptor (GO:0016773, 101), and kinase activity (GO:0016301, 112) (Figure 8; Table S4). A total of 798 up-regulated DEGs were enriched in the Biological Process category, with most up-regulated genes associated with GO terms related to phosphorus metabolism and response to stimuli (Figure 8; Table S4).

The GO analysis of down-regulated DEGs indicated that they were primarily enriched in GO terms related to secondary metabolism, including lignin metabolic process (GO:0009808), catalytic activity (GO:0003824), and phenylpropanoid metabolic process (GO:0009698) (Figure 8B; Table S5).

3.7. Expression Profile of DEGs Associated with the Plant Hormone Signal Transduction Pathways

The KEGG enrichment analysis indicated that up-regulated and down-regulated genes were enriched in the "Plant hormone signal transduction" pathway; hence, the expression of genes related to this pathway was analyzed. In the IAA signaling pathway, a total of 51 DEGs were identified (Figure 9). Of these DEGs, two *auxin influx carriers* (*AUX1*) were identified, with one (Cg8g001890) being up-regulated in abnormal flowers. Seventeen *auxin-responsive proteins* (*AUX/IAA*) were identified, with nine of them up-regulated in abnormal flowers. One *IAA transport inhibitor response* (*TIR1*, Cg2g041270) was identified in the DEGs, and this gene was down-regulated in abnormal flowers. Two *auxin response factors* (*ARF*, Cg3g023780 and Cg5g040580) were differentially expressed between the two types of petals, and both were up-regulated in abnormal flowers. Of the six differentially expressed *auxin-responsive GH3* genes, only one (Cg2g014520) was up-regulated in abnormal flowers. In addition, 23 auxin-responsive *Small Auxin-Up RNA (SAUR)* genes were differentially expressed, of which 16 were up-regulated in abnormal flowers.

In the CTK signaling pathway, a total of 11 DEGs were identified (Figure 9). Of these, one *CTK receptor* (*CRE1*, Cg2g028980), four *histidine-containing phosphotransfer proteins* (*AHPs*: Cg2g030480, Cg5g036350, Cg8g017880, and Cg9g003870), three *B-type response regulators* (*B-ARRs*: Cg4g001620, Cg7g017820, and Cg9g001730), and one *A-type response regulator* (*A-ARR*: Cg5g004380) were up-regulated in abnormal flowers.

In the BR signaling pathway, a total of 8 DEGs were identified, with 7 of them up-regulated in abnormal flowers (Figure 9). These include one *BR-signaling kinase* (*BSK*, Cg5g042160), one *protein brassinosteroid insensitive 2* (*BIN2*, Cg2g008870), three *xyloglucosyl*

transferase TCH4 genes (Cg4g022120, Cg4g022130, Cg4g022140), and two *cyclin D3* (*CYCD3*) genes (Cg1g005860 and Cg8g004060).

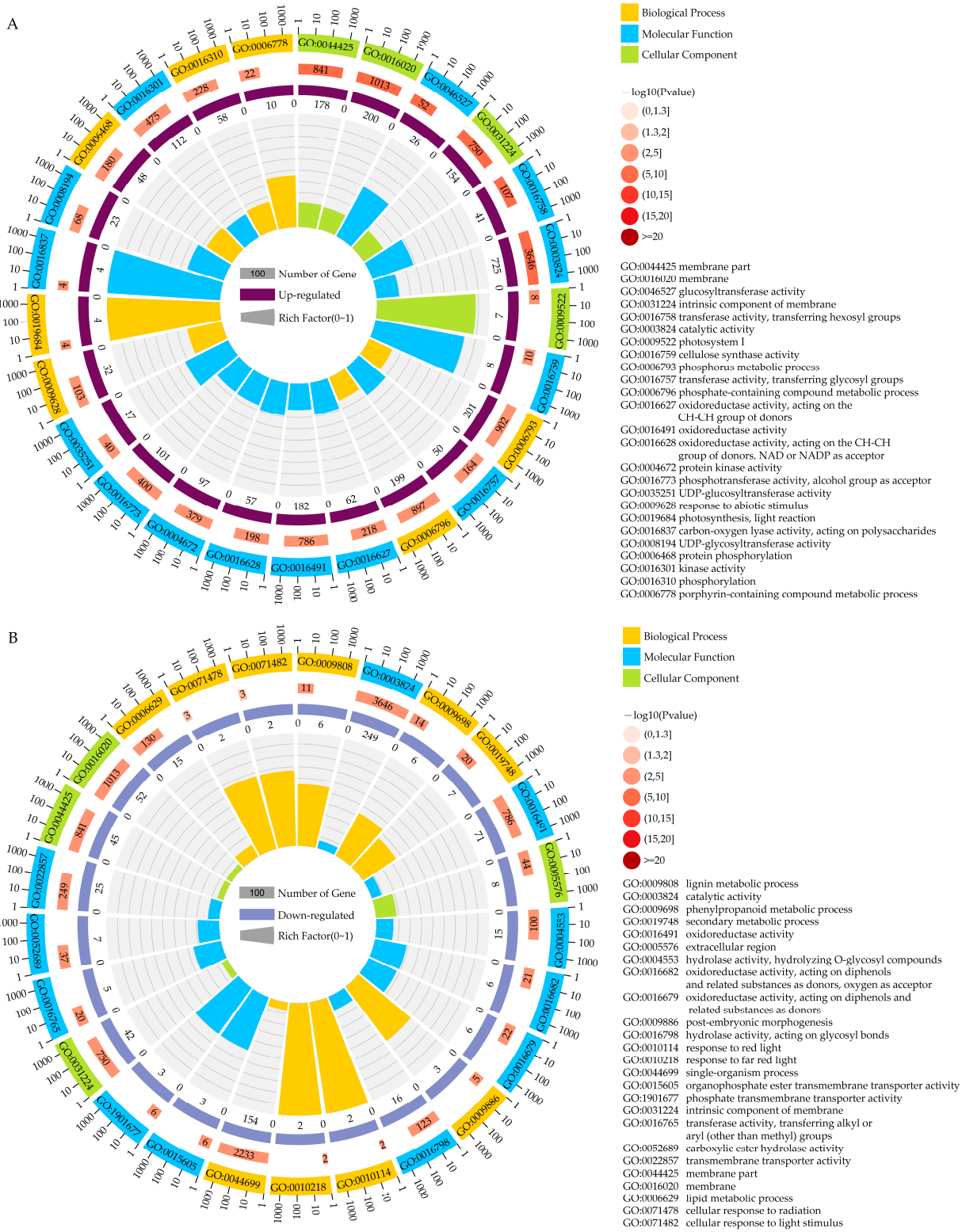


Figure 8. Top 25 Gene Ontology (GO) terms enriched among up-regulated (**A**) and down-regulated (**B**) differentially expressed genes. The innermost bar chart represents the enrichment factor for each GO term, defined as the proportion of differentially expressed genes relative to the total number of genes annotated to that term.

In the ET signaling pathway, a total of 3 DEGs were identified, all of which were up-regulated in abnormal flowers (Figure 9). These include one *ET receptor* (*ETR*, Cg5g037800), one *EIN3-binding F-box protein* (*EBF1_2*, Cg4g007230), and one *ET-responsive transcription factor 1* (*ERF1*, Cg5g034050).

In the GA signaling pathway, a total of 4 DEGs were identified, including 1 *gibberellin receptor* (*GID1*, Cg2g030540), 1 *DELLA protein* (*EBF1_2*, Cg2g033500), and 3 *phytochrome-interacting factor 4* (*PIF4*) genes (Cg5g032930, Cg7g012190, and Cg5g013200) (Figure 9).

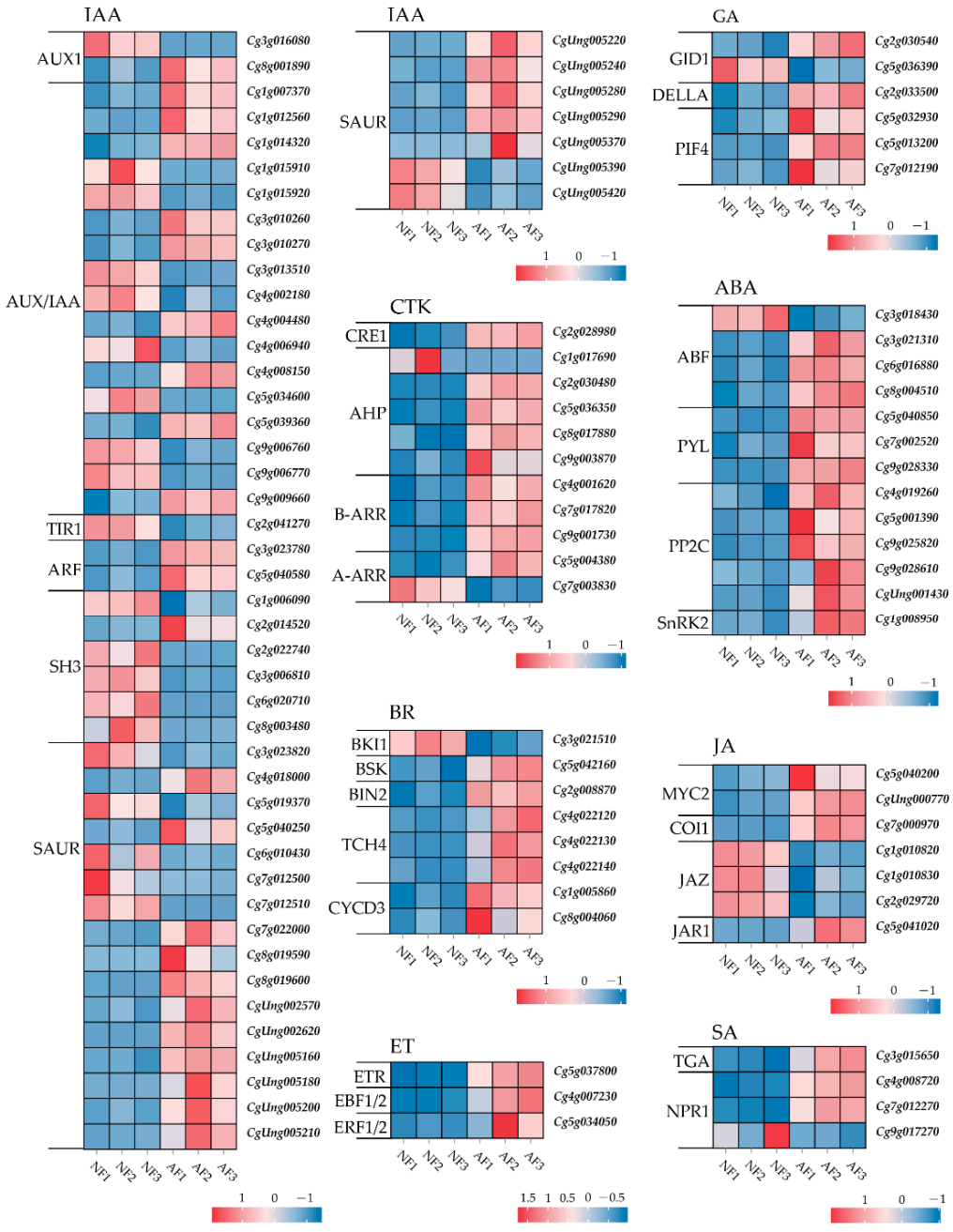


Figure 9. Heatmap of differentially expressed genes in plant hormone signal transduction pathways. The heatmap displays Z-score-normalized FPKM values. NF: Normal flowers; AF: Abnormal flowers.

In the ABA signaling pathway, a total of 13 DEGs were identified, with 12 of them up-regulated in abnormal flowers (Figure 9). These include 3 *ABA-responsive element binding factors* (*ABF*), 3 *ABA receptors* (*PYL*), 5 protein *phosphatase 2C* (*PP2C*), and 1 *serine/threonine-protein kinase* (*SnRK2*).

In the JA signaling pathway, three negative regulators of the pathway, the *jasmonate ZIM domain-containing proteins* (*JAZ*: Cg1g010820, Cg1g010830, Cg2g029720), were down-regulated in the abnormal flowers (Figure 6). Other positive regulators of the JA pathway were up-regulated in the abnormal flowers, including two transcription factors *MYC2* (Cg5g040200, CgUng000770), one *coronatine-insensitive protein 1* (*COI-1*, Cg7g000970), and one *JA-amino synthetase* (*JAR1*, Cg5g041020).

In the SA signaling pathway, one regulatory protein, *Nonexpressor of Pathogenesis-Related Genes 1* (*NPR1*: Cg4g008720, Cg7g012270), and one transcription factor, *TGACG-binding factor* (*TGA*, Cg3g015650), were up-regulated in abnormal flowers (Figure 9).

3.8. Expression Profile of DEGs Associated with the Mitogen-Activated Protein Kinase (MAPK) Signaling Pathway-Plant

The GO analysis revealed that the DEGs were enriched in "protein kinase activity" and "response to stimulus". Consequently, we analyzed the expression characteristics of genes associated with the "MAPK signaling pathway-plant". A total of 33 DEGs were mapped to this pathway, with 28 genes being up-regulated in the abnormal flowers (Figure 10). These included four transcription factors: *MYC2* (Cg5g040200, CgUng000770), *WRKY29* (Cg5g002150), and *ERF1* (Cg5g034050).

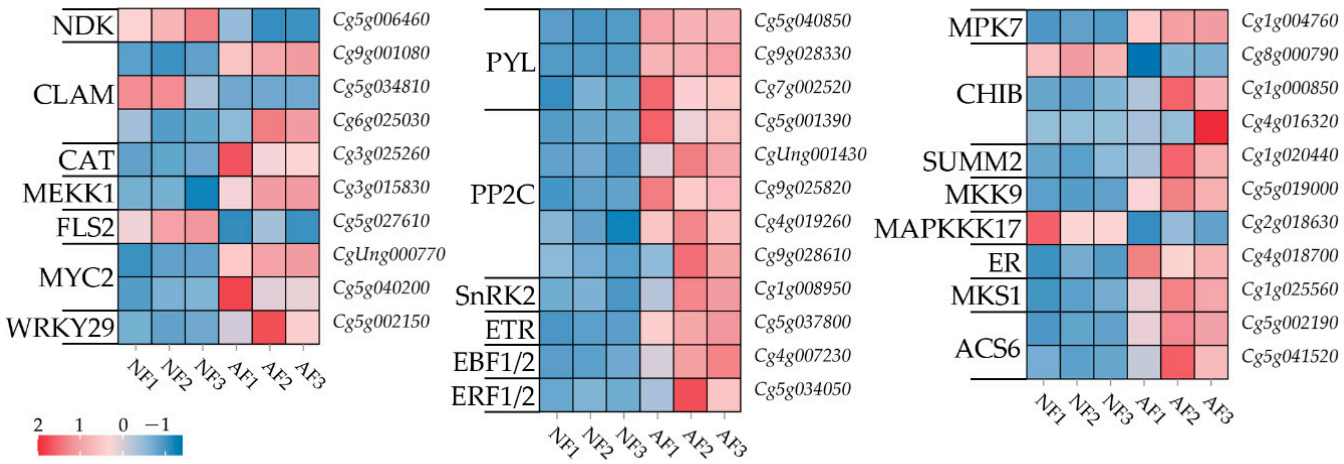


Figure 10. Heatmap of differentially expressed genes in Mitogen-Activated Protein Kinase signaling pathway-Plant. The heatmap displays Z-score-normalized FPKM values. NF: Normal flowers; AF: Abnormal flowers.

3.9. Expression Profile of DEGs Associated with Cell Division

Morphological observation revealed that the petal thickening of *Citrus grandis* 'Huazhou' is primarily attributable to an increase in cell layers. Based on this, the expression of genes involved in cell division was analyzed. Among the cell cycle and division-related genes, 20 were differentially expressed (Figure 11). Among these, 11 cell cycle-related genes were up-regulated in the abnormal flowers, including 1 *cyclin-dependent kinases regulatory subunit 1* (*CKS1*), 3 *Cyclin-U*, 6 *Cyclin-U*, and 1 cell division control protein 2 (*CDC2*). Additionally, 4 cell division-related genes were also up-regulated in the abnormal flowers, including 1 *peptidyl-prolyl cis-trans isomerase CYP28*, 1 *CLIP-associated protein*, 1 *mitotic checkpoint protein BUB3.2*, and 1 *mitogen-activated protein kinase*.

Regarding DNA replication, a critical process in cell division, five genes involved in DNA replication were found to be differentially expressed, with four of them (including MCM) up-regulated in the abnormal flowers (Figure 11).

Concerning cell wall relaxation and expansion, a key step in cell division, twelve Expansin genes showed differential expression, with eleven of them up-regulated in the

abnormal flowers (Figure 11). Additionally, four *Pectinesterase* (*PE*) genes, which are involved in pectin degradation in the cell wall, were up-regulated in the abnormal flowers. Eleven *xyloglucan endotransglucosylase/hydrolase* (*XTH*) genes, which are involved in cellulose degradation in the cell wall, were differentially expressed, with six of them up-regulated in the abnormal flowers.

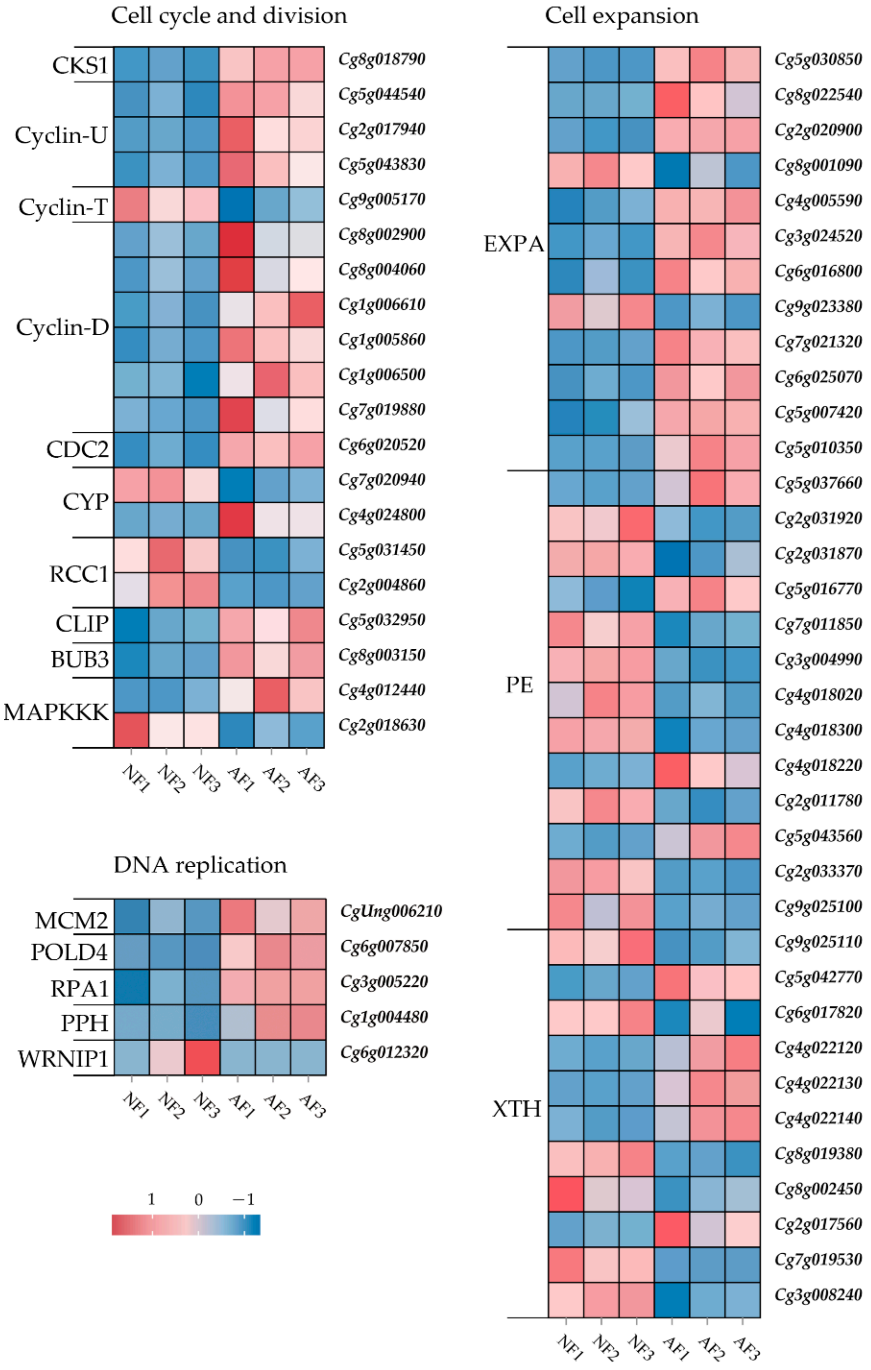


Figure 11. Heatmap of differentially expressed genes in cell division. The heatmap displays Z-score-normalized fragments per kilobase of transcript per million mapped reads (FPKM) values. NF: Normal flowers; AF: Abnormal flowers.

3.10. Expression Profile of DEGs Associated with Energy Metabolism and Material Metabolism

The chloroplast is a crucial energy metabolism site in plant cells, converting light energy into chemical energy. In the porphyrin and chlorophyll metabolism pathway, there were 23 DEGs, with 16 up-regulated in abnormal flowers (Figure 12), including the

key enzyme, *chlorophyll synthase* (Cg6g009290) (Table S6). In contrast, genes encoding Chlorophyll b Reductase (Cg9g019360, Cg9g019380), which catalyzes the conversion of Cb to Ca, and the *STAY-GREEN* gene (Cg5g009510), which catalyzes Ca degradation, were down-regulated in abnormal flowers (Table S6). In the photosynthesis pathway, all DEGs involved in photosystem II (PSII), photosystem I (PSI), cytochrome b6/f complex (Cytb6/f), and photosynthetic electron transporter synthesis were up-regulated in abnormal flowers (Figure 12). Of the four differentially expressed ATPase genes, three were up-regulated in abnormal flowers. In the photosynthesis—antenna proteins pathway, 15 DEGs encoding light-harvesting chlorophyll complexes (LHC) were up-regulated in abnormal flowers (Figure 12). In the carbon fixation in photosynthetic organism pathway, there were 24 DEGs, with 20 up-regulated in abnormal flowers (Figure 12), including genes encoding key enzymes of the Calvin cycle: ribulose-1,5-bisphosphate carboxylase/oxygenase (RuBisCO) (Cg6g019580) and phosphoribulokinase (Cg3g008680) (Table S6).

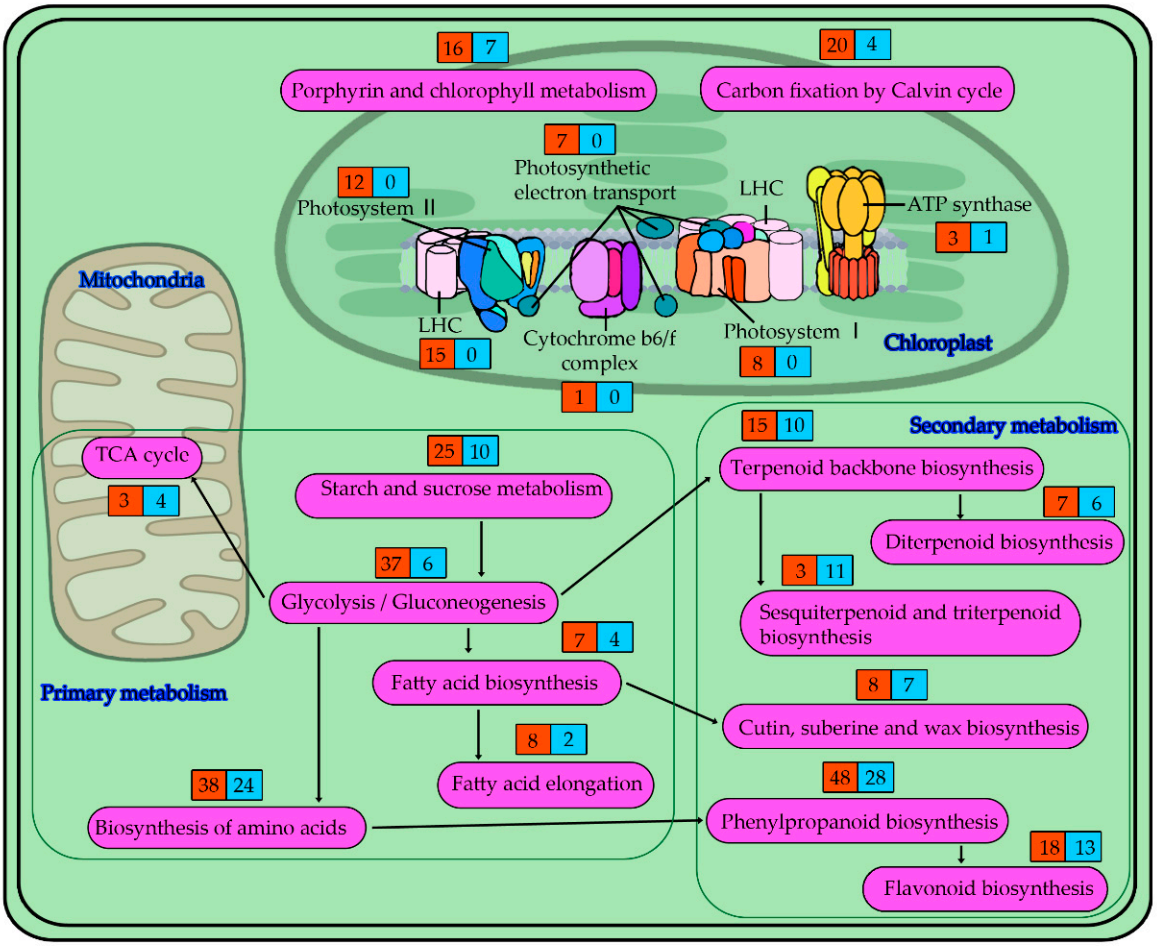


Figure 12. The transcription analysis of energy and material metabolism. The numbers in the boxes indicate the number of differentially expressed genes (DEGs), with orange and blue boxes representing up-regulated and down-regulated expression, respectively.

In the carbon metabolism-related pathways, there were 35 DEGs in the starch and sucrose metabolism pathway (25 up-regulated in abnormal flowers). In the glycolysis/gluconeogenesis pathway, there were 43 DEGs (37 up-regulated and six down-regulated in abnormal flowers), including the gene encoding hexokinase (Cg5g016720) with down-regulated expression. The genes encoding the pyruvate dehydrogenase E1 component (Cg2g044960) and pyruvate dehydrogenase E2 component (Cg3g020270), which are involved in acetyl-CoA synthesis, were down-regulated in abnormal flowers (Table S6). In

contrast, all 16 differential genes encoding enzymes related to the conversion of pyruvate to acetaldehyde, ethanol, and acetic acid were up-regulated in abnormal flowers.

The tricarboxylic acid cycle (TCA cycle) is the aerobic oxidation step of sugar in mitochondria, with seven DEGs, including three DEGs up-regulated in abnormal flowers: *malate dehydrogenase* (Cg4g010670), *aconitate hydratase* (Cg1g001140), and *succinyl-CoA synthetase alpha subunit* (Cg7g013910) (Table S6). In the amino acid biosynthesis pathway, there were a total of 62 DEGs, with 38 up-regulated in abnormal flowers. Additionally, in abnormal flowers, 7 out of 11 DEGs in the fatty acid biosynthesis pathway and 8 out of 10 DEGs in the fatty acid elongation pathway were up-regulated (Figure 12; Table S6).

Terpenoids are key components influencing the fragrance of *C. grandis* 'Tomentosa' flowers, and they also serve as anti-insect substances. Of the 25 DEGs in the terpenoid backbone biosynthesis pathway, 15 were up-regulated in abnormal flowers. The most significantly up-regulated genes were farnesyl diphosphate synthase (involved in the synthesis of farnesyl diphosphate and geranyl diphosphate) and geranylgeranyl diphosphate synthase (involved in the synthesis of geranylgeranyl diphosphate). In the monoterpenoid biosynthesis pathway, 2 out of 8 DEGs were up-regulated in abnormal flowers, encoding neomenthol dehydrogenase (Cg5g042430, Cg8g018240) for neomenthol synthesis. In the diterpenoid biosynthesis pathway, 7 out of 13 DEGs were up-regulated, whereas down-regulated DEGs were genes mainly related to GA synthesis.

In the sesquiterpenoid and triterpenoid biosynthesis pathway, 3 out of 14 DEGs were up-regulated in abnormal flowers (Figure 12), including the gene encoding the enzyme for farnesal synthesis (NAD+-dependent farnesol dehydrogenase, Cg3g021540), the gene encoding the enzyme for beta-farnesene synthesis (Cg9g012400), and the gene encoding the enzyme for germacrene D synthesis (Cg4g011140) (Table S6).

The biosynthesis of cutin, suberin, and wax is closely related to the plant's ability to resist external pests and diseases. In this pathway, there were 15 DEGs, with eight up-regulated in the abnormal flowers, primarily involving genes responsible for synthesizing 16-feruloyloxypalmitic acid and 16-oxopalmitate (Figure 12; Table S6).

Flavonoids are not only important secondary metabolites in the flowers but also substances that plants use to resist external pests and diseases. In the phenylpropanoid biosynthesis pathway, out of 76 DEGs, 48 were up-regulated in abnormal flowers. The most significantly up-regulated genes included those encoding cinnamyl-alcohol dehydrogenase (with four up-regulated DEGs) and Peroxidase (POD, with 28 DEGs), which were involved in lignin biosynthesis (Table S6). In the flavonoid biosynthesis pathway, 18 out of 31 DEGs were up-regulated in abnormal flowers (Figure 12), including genes involved in the synthesis of afzelechin, gallocatechin, phlorizin, and catechin (Table S6).

3.11. Validation of Transcriptome Data by Quantitative Real-Time PCR

To verify the accuracy of the transcriptome data, 12 DEGs involved in hormone biosynthesis and signal transduction, flavonoid biosynthesis, volatile compound biosynthesis, and cell wall formation were selected, and their expression levels were analyzed by qRT-PCR. Among these, eight DEGs, *chitinase* (Cg4g016320), *POD* (Cg2g001400), *malate dehydrogenase* (Cg8g002200), *SAUR36-like* (Cg8g019600), *glyceraldehyde-3-phosphate dehydrogenase A* (Cg2g009300), *Myb4* (Cg6g02514), *caffeoyl-CoA O-methyltransferase 5-like* (Cg1g017410), and *XTH22-like* (Cg4g022120), were up-regulated in abnormal flowers. In contrast, four DEGs, *(3S,6E)-nerolidol synthase 1* (Cg2g040890), *IAA8-like* (Cg3g013510), *(R)-limonene synthase 1-like* (Cg2g040870), and *gibberellin 2-β-dioxygenase 8 isoform X3* (Cg2g040470), were down-regulated in abnormal flowers. The relative expression patterns of these 12 DEGs were consistent with the corresponding FPKM values obtained from the transcriptome analysis, confirming the reliability of the RNA-seq data (Figure 13).

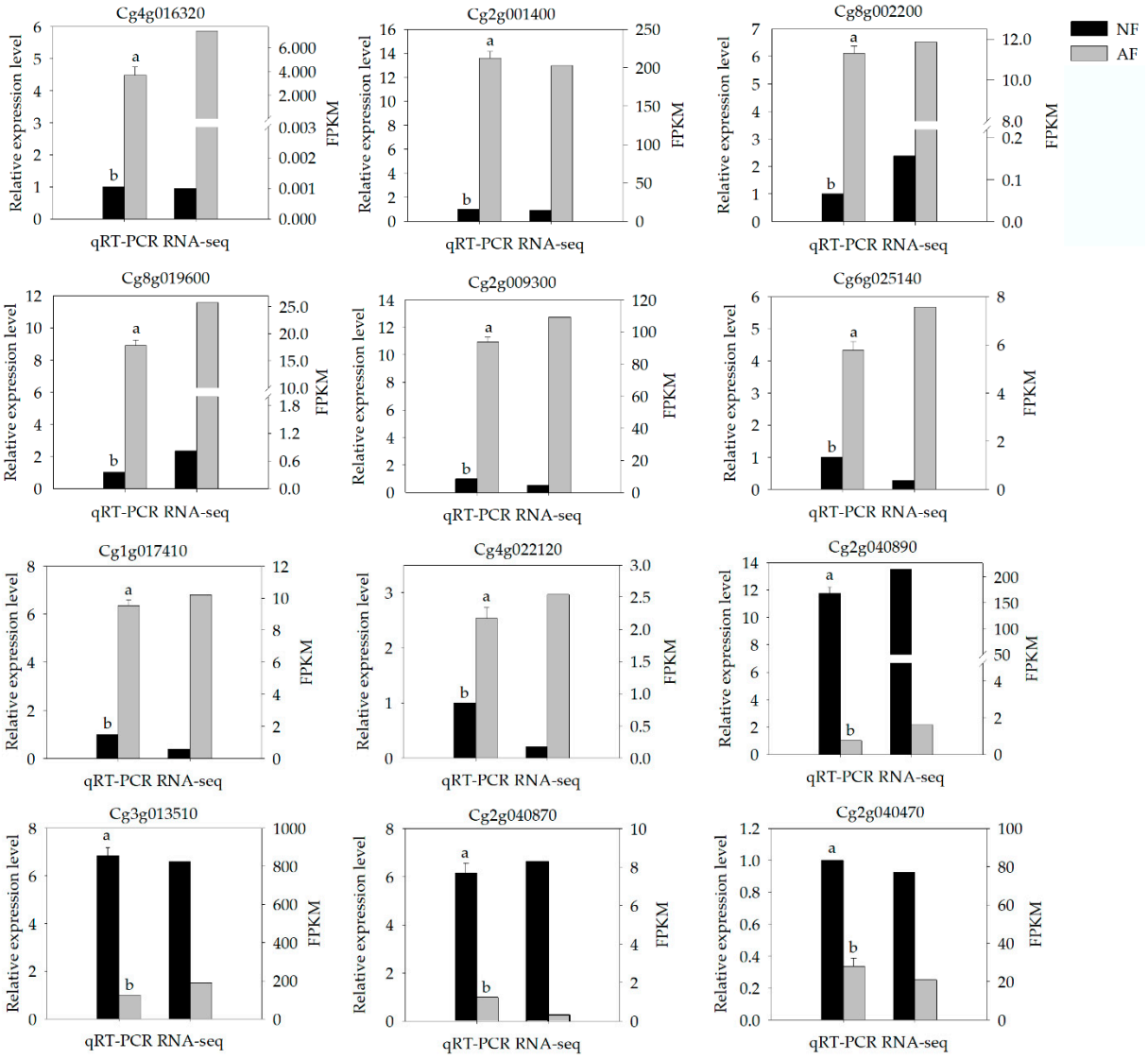


Figure 13. The fragments per kilobase of transcript per million mapped reads (FPKM) values and real-time quantitative reverse transcription polymerase chain reaction results of the 12 differentially expressed genes. Different lowercase letters denote statistically significant differences (Duncan's test, $p < 0.05$).

4. Discussion

Infestation of *C. grandis* 'Tomentosa' flowers by *C. citri* induces abnormal floral development, typified by petal thickening that impairs anthesis and results in a lantern-like morphology, a phenotype analogous to gall formation, in which pests manipulate host developmental and transcriptional programs [40–43]. Such manipulation perturbs plant defense responses [44,45], hormone signaling [46,47], cell cycle regulation, cell wall and cytoskeleton organization [47–49], and metabolic processes [50,51], ultimately driving profound morphological remodeling. This process entails intricate plant–pest interactions and complex inter- and intracellular molecular and physiological networks [40–43]. Morphological analyses revealed that *C. citri* infestation increased the number of transverse cell layers in *C. grandis* 'Tomentosa' petals, leading to petal thickening and lantern-like flower formation. Concomitantly, infestation altered petal levels of plant hormones, chlorophyll, and total flavonoids. Transcriptomic profiling showed that up-regulated genes in abnormal flowers were predominantly enriched in plant hormone signaling pathways, carbon metabolism, and phenylpropanoid biosynthesis, as well as GO terms associated with regu-

lation of enzyme activity, phosphorus metabolism, and responses to stimuli. Collectively, *C. citri*-mediated abnormal floral development in *C. grandis* 'Tomentosa' involves complex molecular and physiological regulation encompassing hormonal signaling, cellular defense, and material metabolism.

Plant hormones are crucial signaling molecules that regulate plant growth [52], development [53], and defense processes [52,54] and play a key role in response to wounding [55]. JA and SA are two key hormones in plant immunity. First, JA confers resistance to biotrophic and hemibiotrophic pathogens and is also involved in plant responses to abiotic stresses, such as soil salinity, injury, and ultraviolet radiation, as well as the biosynthesis of metabolites, such as phytoalexins and terpenoids [56,57]. SA plays a central role in systemic acquired resistance (SAR) in plants, regulating the accumulation of pathogenesis-related proteins and the activation of defense genes [57,58]. Exogenous application of JA and SA can induce resistance to Spodoptera frugiperda in maize [59]. In this study, we found that after infestation by the *C. citri*, the SA content in the petals of abnormal flowers of *C. grandis* 'Tomentosa' was significantly higher than that in normal flowers; accordingly, two *NPR1* genes and one *TGA* gene were up-regulated in abnormal flowers. In contrast, the JA content in the petals of normal flowers was significantly higher than that in abnormal flowers, whereas the positive regulatory genes in the JA signaling pathway, including *JAR1*, *COI1*, and *MYC2*, were up-regulated in abnormal flowers, and the negative regulatory gene *JAZ* was down-regulated. Numerous studies have demonstrated that JA acts as a long-distance signal in the process of SAR [56,57,60]. Therefore, the increase in JA content in normal flowers can remotely up-regulate JA signal transduction in abnormal flowers.

In the MAPK signaling pathway, a total of 33 DEGs were identified, with 28 genes up-regulated in abnormal flowers, including two *MYC2* (Cg5g040200, CgUng000770), one *WRKY29* (Cg5g002150), and one *ERF1* (Cg5g34050). In rice, the MYC2–JAMYB transcriptional cascade enhances resistance to the brown planthopper [61]. NPR1 is a key immune regulator in plants that activates plant immunity under biotic and abiotic stresses, enabling their survival [62,63]. WRKY transcription factors play a crucial role in plant defense responses against herbivory [64]. In rice, OsWRKY45 enhances plant resistance to herbivores by regulating diterpenoid phytoalexins [65]. The *SaERF1* gene can enhance the resistance of *Solidago altissima* to the herbivorous *Spodoptera litura* by increasing the transcription level of defensin genes [66]. *C. citri* can induce JA and SA hormone signaling transduction in *C. grandis* 'Tomentosa' flowers, leading to a series of resistance responses.

The increase in the number of transverse cell layers in the petals is the reason for the thickening of *C. grandis* 'Tomentosa' petals induced by *C. citri*, indicating that the mite induces cell division in the petals. Gall tissues are rich in IAA and CKs [67,68], and exogenous application of CKs combined with IAA can induce gall-like growth in pepper petioles [69]. Therefore, the prevailing hypothesis is that gall formation is triggered by plant hormones such as IAA and CKs. CTK and BR biosynthesis are involved in the regulation of cell division and growth during gall formation induced by the gall wasp, *Hemadas nubilipennis* (Ormyridae) in the highbush blueberry, *Vaccinium corymbosum* (Ericaceae) [70]. In this study, we found that after infestation by the *C. citri*, the contents of IAA and cZ in the petals of abnormal flowers of *C. grandis* 'Tomentosa' were significantly higher than those in normal flowers. IAA, CTK, and BR can regulate cell division and cell wall expansion through their respective signaling pathways [71]. In the IAA hormone signaling transduction, two differentially expressed *ARF* genes were up-regulated in abnormal flowers, and most *AUX/IAA* and *SAUR* genes were also up-regulated. In CTK hormone signaling transduction, all differentially expressed *B-ARR* genes and one *A-ARR* gene were up-regulated in abnormal flowers. In BR hormone signaling transduction, genes involved in cell elongation and division were all up-regulated in abnormal flowers, including three

TCH4 genes and two *CYCD3* genes. In the genes regulating the cell cycle, cell division, and DNA replication, the majority of DEGs were up-regulated in abnormal flowers. Most of the expansion protein genes involved in cell wall extension were also up-regulated in abnormal flowers. *C. citri* can induce the up-regulation of IAA, CTK, and BR signaling pathway genes in petals, thereby promoting the expression of genes related to the cell cycle, cell division, DNA replication, and cell wall expansion, leading to an increase in petal cell number.

After insects parasitize inside plants, they require substantial plant resources for development and reproduction. Many genes involved in carbohydrate and amino acid synthesis are significantly up-regulated in gall tissues [68,72,73]. *C. citri* can up-regulate the expression of chlorophyll biosynthesis-related genes in *C. grandis* 'Tomentosa' petals. Consequently, the contents of Ca and Cb in the petals of abnormal flowers are significantly higher than those in normal flowers, resulting in the green coloration of the petals. Simultaneously, genes associated with the photosynthetic system, Calvin cycle, sugar metabolism, and amino acid synthesis were up-regulated in abnormal flowers. This may be how the *C. citri* enhances photosynthesis in the petals, thereby promoting the accumulation of more carbohydrates and amino acids to provide nutrition for the growth and development of the larvae.

After an insect infestation, plants up-regulate the expression of related genes to produce secondary metabolites, thereby enhancing their immune capacity. These metabolites include terpenoids, flavonoids, lignin, and waxes [68,70,73,74]. *C. citri* can up-regulate the expression of genes involved in the terpenoid backbone and diterpenoid biosynthesis in *C. grandis* 'Tomentosa' petals. Most genes related to the biosynthesis of secondary metabolites, such as cutin, suberin, wax, phenylpropanoids, and flavonoids, were also up-regulated under the induction of the *C. citri*. Meanwhile, the total flavonoid content in the petals of abnormal flowers was also significantly higher than that in normal flowers. This indicates that under *C. citri* infestation, *C. grandis* 'Tomentosa' petals can enhance their resistance to the mite by synthesizing secondary metabolites.

In summary, the findings elucidate the molecular mechanisms underlying the abnormal petal development of *C. grandis* 'Tomentosa' induced by the citrus bud mite, leading to lantern-like flowers. Comprehensive analysis indicated that, under *C. citri* infestation, the IAA, CTK, and BR hormone signaling pathways in petals were activated, promoting the expression of genes associated with the cell cycle, cell division, DNA replication, and cell wall expansion, ultimately increasing petal cell number. *C. citri* also induced the expression of genes involved in chlorophyll biosynthesis, increasing chlorophyll content and enhancing the expression of genes encoding components of the photosynthetic system. This likely promotes photosynthesis and amino acid synthesis, providing nutrients for larval development. Concurrently, plants mounted stress responses to *C. citri* invasion, with most genes in the JA, SA, and MAPK signaling pathways being up-regulated. This, in turn, stimulated the expression of genes involved in the biosynthesis of defense-related compounds, such as terpenoids, flavonoids, lignin, and wax, thereby enhancing petal resistance to the mite (Figure 14). This deepens our understanding of plant–insect interactions and offers valuable references for studying structural abnormalities in plants caused by other insects, such as galls. However, our study has some acknowledged limitations. The research sampled only abnormal and normal flowers at a single time point, lacking a comprehensive analysis of genes throughout the entire petal development cycle. Second, changes in all metabolites in petals were not fully characterized. Future research could adopt a more comprehensive time-series experimental design to systematically analyze changes in hormones, metabolites, and gene expression characteristics throughout the developmental period. This approach would facilitate a deeper understanding of the dynamic interactions

between abnormal petal development and the host plant across multiple developmental stages, thereby elucidating the molecular mechanisms of lantern-like flower formation.

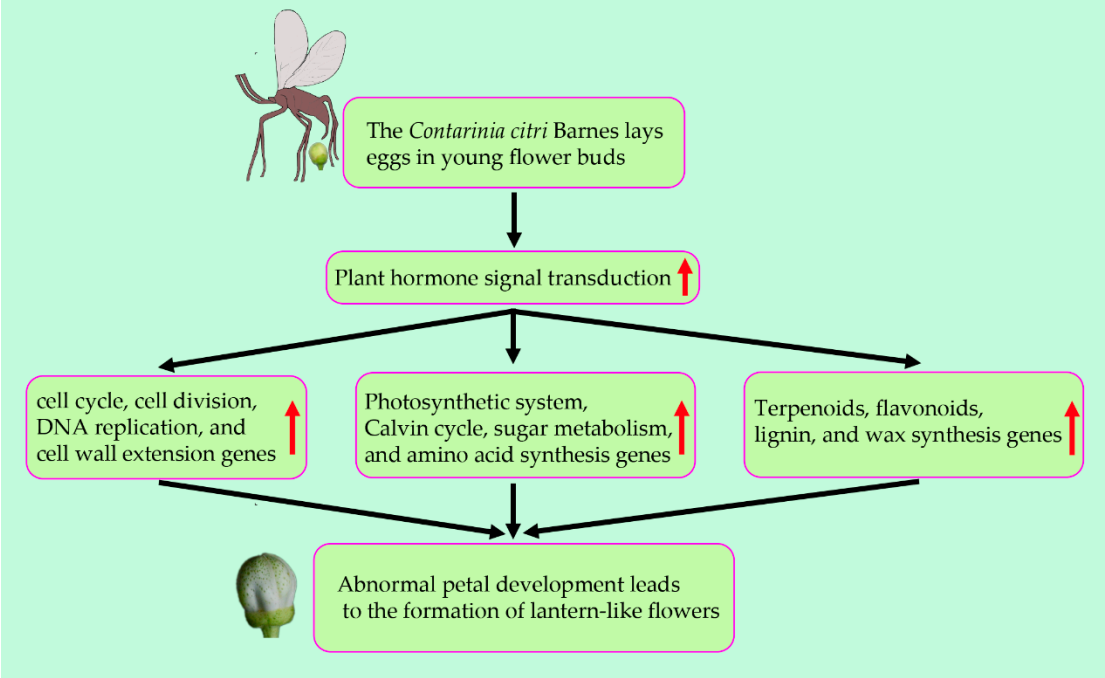


Figure 14. Proposed regulatory model of abnormal petal development in *Citrus grandis* 'Tomentosa' induced by *Contarinia citri* Barnes. Red arrows indicate the up-regulated expression of related genes.

5. Conclusions

Abnormal petal development triggered by *C. citri* infestation is typified by an expanded number of transverse cell layers, elevated levels of SA, IAA, and cZ, enhanced accumulations of chlorophyll and total flavonoids, and the emergence of green spots on the petals. In abnormal flowers, the expression of genes related to photosynthesis, material metabolism, and hormone signaling transduction differs markedly from that in normal petals. This study elucidates the molecular mechanisms underlying abnormal petal development in *C. grandis* 'Tomentosa' induced by *C. citri*, provides a theoretical basis for future pest-resistant breeding of *C. grandis* 'Tomentosa', and lays the groundwork for the development of targeted, environmentally friendly control strategies against *C. citri*. These findings have practical significance for protecting citrus production and mitigating the economic losses caused by this pest.

Supplementary Materials: The following supporting information can be downloaded at: https://www.mdpi.com/article/10.3390/horticulturae12020163/s1, Supplementary Table S1: Gene and primer information used for RT-qPCR. Supplementary Table S2: KEGG enrichment analysis of up-regulated differentially expressed genes. Supplementary Table S3: KEGG enrichment analysis of down-regulated differentially expressed genes. Supplementary Table S4: GO enrichment analysis of up-regulated differentially expressed genes. Supplementary Table S5: GO enrichment analysis of down-regulated differentially expressed genes. Supplementary Table S6: The information on differentially expressed genes (DEGs) in energy metabolism and material metabolism.

Author Contributions: Conceptualization, Q.H. and H.C.; methodology, Q.H. and H.C.; software, Q.H., H.C. and Z.F.; validation, Q.H., H.C. and Y.L.; formal analysis, Y.L. and J.L.; investigation, Q.H., J.L. and Y.L.; resources, X.H.; data curation, Q.H., J.L. and Y.L.; writing—original draft preparation, Q.H., H.C. and Z.F.; writing—review and editing, Y.L., C.W. and X.H.; visualization, Q.H., H.C. and

Z.F.; supervision, C.W. and X.H.; project administration, C.W. and X.H.; funding acquisition, C.W., X.H. and Y.L. All authors have read and agreed to the published version of the manuscript.

Funding: Guangdong Science and Technology Innovation Strategy Special Project (Major Project and Task List) (2023S017086, 2021S0079, 2023S005052), the Science and Technology Planning Project of Maoming (2022S038), 2024 Guangdong Provincial Science and Technology Support Program for the "Hundred-Thousand-Ten Thousand Project" (2024003), Talent Introduction Project of Guangdong University of Petrochemical Technology (2024rcyj1028).

Data Availability Statement: The raw sequence data reported in this paper have been deposited in the Genome Sequence Archive (Genomics, Proteomics and Bioinformatics 2021) at the National Genomics Data Center (Nucleic Acids Res 2022), China National Center for Bioinformation/Beijing Institute of Genomics, Chinese Academy of Sciences (GSA: CRA019385), and are publicly accessible at https://ngdc.cncb.ac.cn/gsa (accessed on 4 October 2024). The data are presented in the article and Supplementary Materials.

Acknowledgments: We thank Guangzhou Genedenovo Biotechnology Co., Ltd. for providing the methods for partial data analysis.

Conflicts of Interest: The authors declare no conflicts of interest.

Abbreviations

The following abbreviations are used in this manuscript:

ECG	Exocarpium Citri Grandis
IAA	Indole-3-acetic acid
JA	Jasmonic acid
CTK	Cytokinins
SA	Salicylic acid
ET	Ethylene
ABA	Abscisic acid
NF	Normal flowers
AF	Abnormal flowers
qRT-PCR	Quantitative reverse transcription polymerase chain reaction
Ca	Chlorophyll a
Cb	Chlorophyll b
FC	Fold change
GO	Gene Ontology
KEGG	Kyoto Encyclopedia of Genes and Genomes
PCA	Principal component analysis
FPKM	Fragments per kilobase of transcript per million mapped reads
DEG	Differentially expressed gene
SAR	Systemic acquired resistance

References

1. Han, H.B.; Li, H.; Hao, R.L.; Chen, Y.F.; Ni, H.; Li, H.H. One-step column chromatographic extraction with gradient elution followed by automatic separation of volatiles, flavonoids and polysaccharides from *Citrus grandis*. *Food Chem.* **2014**, *145*, 542–548. [CrossRef] [PubMed]
2. Committee National Pharmacopoeia. *Pharmacopoeia of People's Republic of China*; China Medical Science Press: Beijing, China, 2020.
3. Xu, Z.; Li, J.; Zhou, K.; Wang, K.; Hu, H.; Hu, Y.; Gao, Y.; Luo, Z.; Huang, J. Exocarpium Citri Grandis ameliorates LPS-induced acute lung injury by suppressing inflammation, NLRP3 inflammasome, and ferroptosis. *J. Ethnopharmacol.* **2024**, *329*, 118162. [CrossRef]
4. Deng, G.; Liu, C.; Zhao, J.; Wang, M.; Li, Y.; Yang, M.; Ye, H.; Li, J.; Qin, M.; Wu, C.; et al. Exocarpium Citri Grandis alleviates the aggravation of NAFLD by mitigating lipid accumulation and iron metabolism disorders. *J. Ethnopharmacol.* **2023**, *313*, 116559. [CrossRef] [PubMed]

5. Li, D.; Xiao, G.; Chen, W.; Zeng, X.; Cao, L.Z.; Chen, Z. Metabolomic-based investigation of Yinlan alleviating hyperlipidemia by inhibiting blood stasis and phlegm turbidity through the PXR-CYP3A4-ABCB1-FXR pathway. *Arab. J. Chem.* **2022**, *15*, 104272. [CrossRef]
6. Liu, G.; Li, S.; Zhang, N.; Wei, N.; Wang, M.; Liu, J.; Xu, Y.; Li, Y.; Sun, Q.; Li, Y.; et al. Sequential grade evaluation method exploration of Exocarpium Citri Grandis (Huajuhong) decoction pieces based on "network prediction → grading quantization → efficacy validation". *J. Ethnopharmacol.* **2022**, *291*, 115149. [CrossRef]
7. Kong, F.; Ding, Z.; Zhang, K.; Duan, W.; Qin, Y.; Su, Z.; Bi, Y. Optimization of extraction flavonoids from Exocarpium Citri Grandis and evaluation its hypoglycemic and hypolipidemic activities. *J. Ethnopharmacol.* **2020**, *262*, 113178. [CrossRef]
8. Chen, M.; Wang, J. Polysaccharides from Exocarpium Citri Grandis: Graded ethanol precipitation, structural characterization, inhibition of α-glucosidase activity, anti-oxidation, and anti-glycation potentials. *Foods* **2025**, *14*, 791. [CrossRef]
9. Harris, K.M.; Yukawa, J. The taxonomic status of the Japanese citrus flower-bud midge, *Contarinia okadai* (Miyoshi) comb. n., and of the citrus blossom midge, *C. citri* Barnes (Diptera: Cecidomyiidae). *Bull. Entomol. Res.* **1980**, *70*, 277–285. [CrossRef]
10. Ma, N.; Wang, Y.; Wei, D.; Yu, Y.; Mu, Y.; Gu, X.; Bu, W.; Jiao, K. Comparison of fruit tree gall midge pests species (Diptera: *Cecidomyiidae*) in Guangxi with morphological and biological key. *Plant Protect.* **2024**, *50*, 246–253. (In Chinese) [CrossRef]
11. Li, M. Harm and control of *Contarinia pyrivora* Ril. *Entomol. Know.* **1959**, *06*, 192. (In Chinese)
12. Shi, D. A study on the Citrus blossom midge, *Contarinia citri* Barnes {Dip., *Cecidomyiidae*}. *Ada Phytophyl. Sin.* **1963**, *2*, 379–385. (In Chinese)
13. Chen, R.; Chen, J.; Yu, J.; Zhou, D.; Qin, R.; Zhang, G.; Yang, G.; Xu, R.; Zhou, F.; Xu, C.; et al. Investigation on pest and natural enemy species of *Citrus grandis* 'Tomentosa'. *J. Chin. Med. Mater.* **2008**, *31*, 1615–1618. (In Chinese) [CrossRef]
14. Qiao, H.; Chen, J.; Xu, C.; Li, X.; Ma, W.; Yu, J.; Chen, H. Spatial distribution of citrus blossom midge in *Citrus grandis* 'Tomentosa' and pathogenicity of metarhizium against its larvae. *J. Chin. Med. Mater.* **2011**, *34*, 852–855. (In Chinese) [CrossRef]
15. Tudi, M.; Daniel Ruan, H.; Wang, L.; Lyu, J.; Sadler, R.; Connell, D.; Chu, C.; Phung, D.T. Agriculture development, pesticide application and its impact on the environment. *Int. J. Environ. Res. Public Health* **2021**, *18*, 1112. [CrossRef]
16. Alengebawy, A.; Abdelkhalek, S.T.; Qureshi, S.R.; Wang, M.Q. Heavy metals and pesticides toxicity in agricultural soil and plants: Ecological risks and human health implications. *Toxics* **2021**, *9*, 42. [CrossRef] [PubMed]
17. Hubbard, C.B.; Murillo, A.C. Behavioral resistance to insecticides: Current understanding, challenges, and future directions. *Curr. Opin. Insect Sci.* **2024**, *63*, 101177. [CrossRef] [PubMed]
18. Zhang, R.; Zhang, M.X.; Chen, Y.; Wang, C.C.; Zhang, C.H.; Heuberger, H.; Li, H.T.; Li, M.H. Future development of Good Agricultural Practice in China under globalization of traditional herbal medicine trade. *Chin. Herb. Med.* **2021**, *13*, 472–479. [CrossRef]
19. Peng, B.; Xie, Y.; Lai, Q.; Liu, W.; Ye, X.; Yin, L.; Zhang, W.; Xiong, S.; Wang, H.; Chen, H. Pesticide residue detection technology for herbal medicine: Current status, challenges, and prospects. *Anal. Sci.* **2024**, *40*, 581–597. [CrossRef]
20. Wang, W.; Xu, J.; Fang, H.; Li, Z.; Li, M. Advances and challenges in medicinal plant breeding. *Plant Sci.* **2020**, *298*, 110573. [CrossRef]
21. Lu, J.; Liu, C. Screening of disease and pest resistant hangbaiju (*Chrysanthemum morifolium*) varieties and their application prospects in green cultivation. *Med. Plant Res.* **2024**, *14*, 345–357. [CrossRef]
22. Liu, Y.X.; Han, W.H.; Wang, J.X.; Zhang, F.B.; Ji, S.X.; Zhong, Y.W.; Liu, S.S.; Wang, X.W. Differential induction of JA/SA determines plant defense against successive leaf-chewing and phloem-feeding insects. *J. Pest Sci.* **2025**, *98*, 1085–1100. [CrossRef]
23. Monte, I. Jasmonates and salicylic acid: Evolution of defense hormones in land plants. *Curr. Opin. Plant Biol.* **2023**, *76*, 102470. [CrossRef]
24. Wang, M.; Wang, Y.; Li, X.; Zhang, Y.; Chen, X.; Liu, J.; Qiu, Y.; Wang, A. Integration of metabolomics and transcriptomics reveals the regulation mechanism of the phenylpropanoid biosynthesis pathway in insect resistance traits in *Solanum habrochaites*. *Hortic. Res.* **2024**, *11*, uhad277. [CrossRef]
25. Luo, Q.; Duan, F.; Song, W. Transcriptomics integrated with metabolomics reveals the defense response of insect-resistant *Zea mays* infested with *Spodoptera exigua*. *Heliyon* **2025**, *11*, e42565. [CrossRef]
26. Gilroy, E.; Breen, S. Interplay between phytohormone signalling pathways in plant defence—Other than salicylic acid and jasmonic acid. *Essays Biochem.* **2022**, *66*, 657–671. [CrossRef]
27. Verma, K.; Kumari, K.; Rawat, M.; Devi, K.; Joshi, R. Crosstalk of jasmonic acid and salicylic acid with other phytohormones alleviates abiotic and biotic stresses in plants. *J. Soil Sci. Plant Nutr.* **2025**, *25*, 4997–5019. [CrossRef]
28. Thaler, J.S.; Humphrey, P.T.; Whiteman, N.K. Evolution of jasmonate and salicylate signal crosstalk. *Trends Plant Sci.* **2012**, *17*, 260–270. [CrossRef]
29. Barah, P.; Bones, A.M. Multidimensional approaches for studying plant defence against insects: From ecology to omics and synthetic biology. *J. Exp. Bot.* **2015**, *66*, 479–493. [CrossRef] [PubMed]

30. Jiao, L.; Bian, L.; Luo, Z.; Li, Z.; Xiu, C.; Fu, N.; Cai, X.; Chen, Z. Enhanced volatile emissions and anti-herbivore functions mediated by the synergism between jasmonic acid and salicylic acid pathways in tea plants. *Hortic. Res.* **2022**, *9*, uhac144. [CrossRef] [PubMed]
31. Yang, M.; Li, H.; Qiao, H.; Guo, K.; Xu, R.; Wei, H.; Wei, J.; Liu, S.; Xu, C. Integrated transcriptome and metabolome dynamic analysis of galls induced by the gall mite *Aceria pallida* on *Lycium barbarum* reveals the molecular mechanism underlying gall formation and development. *Int. J. Mol. Sci.* **2023**, *24*, 9839. [CrossRef] [PubMed]
32. Ge, X.; Fang, S.; Chen, L.; Zhang, D.; Xu, P.; Luo, H.; Wang, L.; Xie, L.; Zhan, R.; Chen, L. Profiling the dynamic alterations of metabolites and phytohormones in response to stress during the post-harvest processing of *Pogostemon cablin* leaves. *Ind. Crops Prod.* **2025**, *230*, 121125. [CrossRef]
33. Lichtenthaler, H.K.; Wellburn, A.R. Determinations of total carotenoids and chlorophylls a and b of leaf extracts in different solvents. *Biochem. Soc. Trans.* **1983**, *11*, 591–592. [CrossRef]
34. Huang, X.; Liu, X.; Wang, Q.; Zhou, Y.; Deng, S.; He, Q.; Han, H. Transcriptomic and targeted metabolome analyses revealed the regulatory mechanisms of the synthesis of bioactive compounds in *Citrus grandis* 'tomentosa'. *PeerJ* **2024**, *12*, e16881. [CrossRef]
35. Langmead, B.; Trapnell, C.; Pop, M.; Salzberg, S.L. Ultrafast and memory-efficient alignment of short DNA sequences to the human genome. *Genome Biol.* **2009**, *10*, R25. [CrossRef]
36. Kim, D.; Langmead, B.; Salzberg, S.L. HISAT: A fast spliced aligner with low memory requirements. *Nat. Methods* **2015**, *12*, 357–360. [CrossRef] [PubMed]
37. Pertea, M.; Pertea, G.M.; Antonescu, C.M.; Chang, T.C.; Mendell, J.T.; Salzberg, S.L. StringTie enables improved reconstruction of a transcriptome from RNA-seq reads. *Nat. Biotechnol.* **2015**, *33*, 290–295. [CrossRef] [PubMed]
38. Love, M.I.; Huber, W.; Anders, S. Moderated estimation of fold change and dispersion for RNA-Seq data with DESeq2. *Genome Biol.* **2014**, *15*, 550. [CrossRef]
39. Livak, K.J.; Schmittgen, T.D. Analysis of relative gene expression data using real-time quantitative PCR and the $2^{-\Delta\Delta CT}$ method. *Methods* **2001**, *25*, 402–408. [CrossRef]
40. Ma, Y.; Şen, Z.B.; Ng, H.P. Plant galls induced by insects: Coordinated developmental reprogramming and defence manipulation. *Curr. Opin. Plant Biol.* **2025**, *86*, 102757. [CrossRef]
41. Le Fevre, R.; Evangelisti, E.; Rey, T.; Schornack, S. Modulation of host cell biology by plant pathogenic microbes. *Annu. Rev. Cell Dev. Biol.* **2015**, *31*, 201–229. [CrossRef]
42. Harris, M.O.; Pitzschke, A. Plants make galls to accommodate foreigners: Some are friends, most are foes. *New Phytol.* **2020**, *225*, 1852–1872. [CrossRef]
43. Takeda, S.; Hirano, T.; Ohshima, I.; Sato, M.H. Recent progress regarding the molecular aspects of insect gall formation. *Int. J. Mol. Sci.* **2021**, *22*, 9424. [CrossRef]
44. Martinson, E.O.; Werren, J.H.; Egan, S.P. Tissue-specific gene expression shows a cynipid wasp repurposes oak host gene networks to create a complex and novel parasite-specific organ. *Mol. Ecol.* **2022**, *31*, 3228–3240. [CrossRef]
45. Shih, T.H.; Chen, J.L.; Huang, M.Y. Transcriptome and 2-DE proteome analyses reveal defense-associated development in the leaf galls induced by psyllids on *Machilus japonica* var. *kusanoi*. *Bot. Stud.* **2025**, *66*, 19. [CrossRef]
46. Hua, J.; Liu, J.; Zhou, W.; Ma, C.; Luo, S. A new perspective on plant defense against foliar gall-forming aphids through activation of the fruit abscission pathway. *Plant Physiol. Biochem.* **2023**, *196*, 1046–1054. [CrossRef] [PubMed]
47. Li, J.; Lu, Z.; Yang, Y.; Hou, J.; Yuan, L.; Chen, G.; Wang, C.; Jia, S.; Feng, X.; Zhu, S. Transcriptome analysis reveals the symbiotic mechanism of Ustilago esculenta-induced gall formation of *Zizania latifolia*. *Mol. Plant Microbe Interact.* **2021**, *34*, 168–185. [CrossRef]
48. Gätjens-Boniche, O.; Jiménez-Madrigal, J.P.; Whetten, R.W.; Valenzuela-Diaz, S.; Alemán-Gutiérrez, A.; Hanson, P.E.; Pinto-Tomás, A.A. Microbiome and plant cell transformation trigger insect gall induction in cassava. *Front. Plant Sci.* **2023**, *14*, 1237966. [CrossRef] [PubMed]
49. Fitoussi, N.; de Almeida Engler, J.; Sichov, N.; Bucki, P.; Sela, N.; Harel, A.; Belausuv, E.; Kumar, A.; Brown Miyara, S. The Minichromosome Maintenance Complex Component 2 (*MjMCM2*) of *Meloidogyne javanica* is a potential effector regulating the cell cycle in nematode-induced galls. *Sci. Rep.* **2022**, *12*, 9196. [CrossRef] [PubMed]
50. Markel, K.; Novak, V.; Bowen, B.P.; Tian, Y.; Chen, Y.C.; Sirirungruang, S.; Zhou, A.; Louie, K.B.; Northen, T.R.; Eudes, A.; et al. Cynipid wasps systematically reprogram host metabolism and restructure cell walls in developing galls. *Plant Physiol.* **2024**, *195*, 698–712. [CrossRef]
51. Guedes, L.M.; Sanhueza, C.; Torres, S.; Figueroa, C.; Gavilán, E.; Pérez, C.I.; Aguilera, N. Gall-inducing *Eriophyes tiliae* stimulates the metabolism of *Tilia platyphyllos* leaves towards oxidative protection. *Plant Physiol. Biochem.* **2023**, *195*, 25–36. [CrossRef]
52. Ali, J.; Mukarram, M.; Ojo, J.; Dawam, N.; Riyazuddin, R.; Ghramh, H.A.; Khan, K.A.; Chen, R.; Kurjak, D.; Bayram, A. Harnessing phytohormones: Advancing plant growth and defence strategies for sustainable agriculture. *Physiol. Plant.* **2024**, *176*, e14307. [CrossRef]

53. Castroverde, C.D.M.; Dina, D. Temperature regulation of plant hormone signaling during stress and development. *J. Exp. Bot.* **2021**, *72*, erab257. [CrossRef]
54. Haghpanah, M.; Namdari, A.; Kaleji, M.K.; Nikbakht-Dehkordi, A.; Arzani, A.; Araniti, F. Interplay between ROS and hormones in plant defense against pathogens. *Plants* **2025**, *14*, 1297. [CrossRef]
55. Cunha, A.F.A.; Rodrigues, P.H.D.; Anghinoni, A.C.; de Paiva, V.J.; Pinheiro, D.G.D.S.; Campos, M.L. Mechanical wounding impacts the growth versus defense balance in tomato (*Solanum lycopersicum*). *Plant Sci.* **2023**, *329*, 111601. [CrossRef]
56. Ghorbel, M.; Brini, F.; Sharma, A.; Landi, M. Role of jasmonic acid in plants: The molecular point of view. *Plant Cell Rep.* **2021**, *40*, 1471–1494. [CrossRef]
57. Martinuz, A.; Sikora, R.A.; Vilchez, S.; Schouten, A. The role of salicylic and jasmonic acid in the induction of resistance in *Arabidopsis thaliana* against *Meloidogyne incognita*. *Physiol. Mol. Plant Pathol.* **2025**, *140*, 102943. [CrossRef]
58. Spoel, S.H.; Dong, X. Salicylic acid in plant immunity and beyond. *Plant Cell* **2024**, *36*, 1451–1464. [CrossRef] [PubMed]
59. Kanwal, B.; Tanwir, S.; Ahmad, F.; Ahmad, J.N. Jasmonic Acid and Salicylic Acid improved resistance against *Spodoptera frugiperda* infestation in maize by modulating growth and regulating redox homeostasis. *Sci. Rep.* **2024**, *14*, 16823. [CrossRef] [PubMed]
60. Sun, T.; Zhang, Y. Short- and long-distance signaling in plant defense. *Plant J.* **2021**, *105*, 505–517. [CrossRef] [PubMed]
61. Liu, M.; Li, H.; Chen, Y.; Wu, Z.; Wu, S.; Zhang, J.; Sun, R.; Lou, Y.; Lu, J.; Li, R. The MYC2-JAMYB transcriptional cascade regulates rice resistance to brown planthoppers. *New Phytol.* **2025**, *246*, 1834–1847. [CrossRef]
62. Kumar, S.; Zavaliev, R.; Wu, Q.; Zhou, Y.; Cheng, J.; Dillard, L.; Powers, J.; Withers, J.; Zhao, J.; Guan, Z.; et al. Structural basis of NPR1 in activating plant immunity. *Nature* **2022**, *605*, 561–566. [CrossRef]
63. Zavaliev, R.; Dong, X. NPR1, a key immune regulator for plant survival under biotic and abiotic stresses. *Mol. Cell* **2024**, *84*, 131–141. [CrossRef]
64. Kundu, P.; Vadassery, J. Role of WRKY transcription factors in plant defense against lepidopteran insect herbivores: An overview. *J. Plant Biochem. Biotechnol.* **2021**, *30*, 698–707. [CrossRef]
65. Akagi, A.; Fukushima, S.; Okada, K.; Jiang, C.J.; Yoshida, R.; Nakayama, A.; Shimono, M.; Sugano, S.; Yamane, H.; Takatsuji, H. WRKY45-dependent priming of diterpenoid phytoalexin biosynthesis in rice and the role of cytokinin in triggering the reaction. *Plant Mol. Biol.* **2014**, *86*, 171–183. [CrossRef] [PubMed]
66. Takafuji, K.; Rim, H.; Kawauchi, K.; Mujiono, K.; Shimokawa, S.; Ando, Y.; Shiojiri, K.; Galis, I.; Arimura, G.I. Evidence that ERF transcriptional regulators serve as possible key molecules for natural variation in defense against herbivores in tall goldenrod. *Sci. Rep.* **2020**, *10*, 5352. [CrossRef] [PubMed]
67. Body, M.J.A.; Zinkgraf, M.S.; Whitham, T.G.; Lin, C.H.; Richardson, R.A.; Appel, H.M.; Schultz, J.C. Heritable phytohormone profiles of poplar genotypes vary in resistance to a galling aphid. *Mol. Plant Microbe Interact.* **2019**, *32*, 654–672. [CrossRef]
68. Wang, W.; Guo, W.; Tang, J.; Li, X. Phytohormones in galls on eucalypt trees and in the gall-forming wasp *Leptocybe invasa* (Hymenoptera: *Eulophidae*). *Agric. Forest Entomol.* **2022**, *24*, 609–617. [CrossRef]
69. Bartlett, L.; Connor, E.F. Exogenous phytohormones and the induction of plant galls by insects. *Arthropod Plant Interact.* **2014**, *8*, 339–348. [CrossRef]
70. Teresi, S.J.; Body, M.J.A.; Fulton, A.; Platts, A.E.; Colle, M.; Fanning, P.D.; Perkins, J.A.; Amadeu, R.R.; Benevenuto, J.; Munoz, P.; et al. Deciphering the underlying genetics of galling resistance to the blueberry stem gall wasp in northern highbush blueberry. *Hortic. Res.* **2025**, *12*, uhaf197. [CrossRef]
71. Takatsuka, H.; Umeda, M. Hormonal control of cell division and elongation along differentiation trajectories in roots. *J. Exp. Bot.* **2014**, *65*, 2633–2643. [CrossRef]
72. Martinson, E.O.; Hackett, J.D.; Machado, C.A.; Arnold, A.E. Metatranscriptome analysis of fig flowers provides insights into potential mechanisms for mutualism stability and gall induction. *PLoS ONE* **2015**, *10*, e0130745. [CrossRef] [PubMed]
73. Dsouza, M.R.; Ravishankar, B.E. Nutritional sink formation in galls of *Ficus glomerata* Roxb. (Moraceae) by the insect *Pauropsylla depressa* (Psyllidae, Hemiptera). *Trop. Ecol.* **2014**, *55*, 129–136.
74. Marchiosi, R.; Dos Santos, W.D.; Constantin, R.P.; de Lima, R.B.; Soares, A.R.; Finger-Teixeira, A.; Mota, T.R.; de Oliveira, D.M.; Foletto-Felipe, M.P.; Abrahão, J.; et al. Biosynthesis and metabolic actions of simple phenolic acids in plants. *Phytochem. Rev.* **2020**, *19*, 865–906. [CrossRef]

Disclaimer/Publisher's Note: The statements, opinions and data contained in all publications are solely those of the individual author(s) and contributor(s) and not of MDPI and/or the editor(s). MDPI and/or the editor(s) disclaim responsibility for any injury to people or property resulting from any ideas, methods, instructions or products referred to in the content.